

# 000 TRANSFORMERS LEARN LATENT MIXTURE MODELS 001 002 IN-CONTEXT VIA MIRROR DESCENT 003 004

005 **Anonymous authors**

006 Paper under double-blind review

## 007 008 ABSTRACT 009

011 Sequence modelling requires determining which past tokens are causally relevant  
012 from the context and their importance: a process inherent to the attention layers  
013 in transformers, yet whose underlying learned mechanisms remain poorly under-  
014 stood. In this work, we formalize the task of estimating token importance as an  
015 in-context learning problem by introducing a novel framework based on Mixture  
016 of Transition Distributions, whereby a latent variable, whose distribution is param-  
017 eterized by a set of unobserved mixture weights, determines the influence of past  
018 tokens on the next. To correctly predict the next token, transformers need to learn  
019 the mixture weights in-context. **We demonstrate that transformers can implement**  
020 **Mirror Descent to learn the mixture weights from the context.** To this end, we give  
021 **an explicit construction of a three-layer transformer that exactly implements one**  
022 **step of Mirror Descent and prove that the resulting estimator is a first-order ap-**  
023 **proximation of the Bayes-optimal predictor.** Corroborating our construction and  
024 **its learnability via gradient descent, we empirically show that transformers trained**  
025 **from scratch converge to this solution: attention maps match our construction, and**  
026 **deeper models’ performance aligns with multi-step Mirror Descent.**

## 027 1 INTRODUCTION

029 In recent years, Machine Learning has been transformed by large language models (LLMs). These  
030 massive, complex models achieve unprecedented performance across diverse tasks beyond text gen-  
031 eration (Bubeck et al., 2023). A striking example is in-context learning (ICL) (Brown et al., 2020;  
032 Min et al., 2022), where models adapt to new tasks using only examples in the prompt without  
033 parameter updates. Mechanistic interpretability has made significant strides in explaining this phe-  
034 nomenon, revealing that transformers can implement computational circuits (Elhage et al., 2021;  
035 Olsson et al., 2022; D’Angelo et al., 2025) that mimic known algorithms. For instance, in set-  
036 tings like linear regression, they learn to implement gradient-based optimization (Garg et al., 2022;  
037 Akyürek et al., 2022; Von Oswald et al., 2023a;b; Zhang et al., 2023; Ahn et al., 2023; Mahankali  
038 et al., 2024), while for Markov Chains, they implement counting-based estimators for the transition  
039 probabilities (Nichani et al., 2024; Edelman et al., 2024; Bietti et al., 2023a; Rajaraman et al., 2024;  
040 Ildiz et al., 2024; Sveté & Cotterell, 2024; Chen et al., 2024). However, these successes are con-  
041 fined to problems where all the sequences rely on the same, fixed causal structure: the relationship  
042 between tokens is static. For instance, in the case of regression, the model only needs to learn that  
043 every even token depends on the previous odd token; in Markov chains, it learns that the next token  
044 depends only on the previous one.

045 Real-world sequential data, particularly language, defies such simplicity. The meaning of a sentence  
046 arises not from the fixed sequence of word meanings, but from the dynamic causal links between the  
047 words that must be inferred from the context. These underlying structures, which are fundamental  
048 to language, are latent variables hidden from direct observation. Consider the sentence in Figure 1.  
049 To predict the final action, a model cannot rely on simple recency. It must infer a latent structure:  
050 that “dog” is the agent, “ball” is the relevant object, and “bird” is a distractor. The influence of a past  
051 token is not merely a function of its position, but of its inferred role. This ability to infer and reason  
052 over unobserved variables, be it syntactic roles, speaker intent, or the causal topic of a discourse, is a  
053 hallmark of intelligence. A robust model must therefore move beyond fixed dependencies and learn  
054 to infer this latent structure, dynamically identifying which tokens are causally relevant in a given  
055 context. These considerations give rise to the core question of this paper:

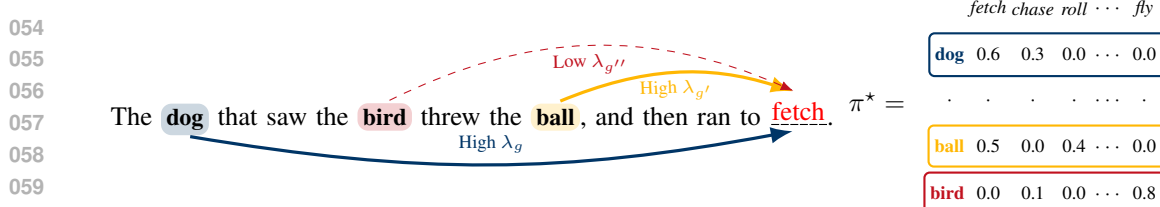


Figure 1: To predict the final word, the model must infer the causal relevance of past tokens. Our MTD framework models this by separating a static, context-free unigram ( $\pi^*$ ) from dynamic, context-dependent weights ( $\lambda$ ) that are inferred in-context. The model learns to assign high weights to the causally relevant positions ('dog') and ('ball'), activating their respective slices of the unigram (e.g.,  $\pi^*(\text{dog}, \cdot)$ ) favouring verbs like *fetch* or *chase*. Conversely, a low weight is assigned to the distractor ('bird'), suppressing its influence.

Can transformers infer latent structures in-context, and what algorithm do they learn?

To investigate this question, we introduce a synthetic task based on the Mixture of Transition Distributions (MTD) model (Raftery, 1985; André Berchtold, 2002). This framework recasts token-importance estimation as learning latent mixture weights in-context. While prior work have used mixture models in regressions (Pathak et al., 2024) or HMMs (Xie et al., 2022) to study ICL, they did not unveil the mechanism through which transformers learn to infer the latent mixture weights.

We make the following contributions:

(I) A framework for ICL based on latent variables using MTD: we create a synthetic task that frames the estimation of the influence of past tokens as learning latent mixture weights in-context. (II) **We identify Mirror Descent as the algorithm transformers can implement to solve this task and provide a construction of a 3-layer transformer that exactly implements one-step of this algorithm.** (III) We empirically demonstrate that transformers trained with Adam actually learn this estimator and the learned attention patterns match our construction and that deeper models match multi-step MD. (IV) We prove that this estimator is an approximation to the Bayes-optimal solution. Taken together, our results extend the gradient-based interpretation of ICL beyond the regression setting. We show for the first time that the same algorithmic perspective holds also in sequential domains over finite sets of discrete tokens. **Our results reveal that Transformers effectively can implement mirror descent to in-context learn latent parameters of Markov-chain tasks, providing a gradient-based explanation of ICL in sequence modeling.** We defer to the Appendix C a more detailed discussion of related work.

**Why MTD?** Our choice of the MTD model is motivated by the desire to capture both in-weight and in-context learning in a single, controlled setting. In contrast to much of the ICL literature, where tasks are designed so that nearly all useful structure must be inferred from the prompt (e.g., gradient-descent ICL in linear regression or counting estimators for simple Markov chains), our setup explicitly assumes that some statistical structure, namely the transition matrix  $\pi^*$ , can be stored in the model’s weights during pretraining and reused at inference time, while the mixture weights  $\lambda$  are inferred and adapted in-context from a single sequence. This mirrors a plausible regime for large language models, which cannot memorize full high-order  $n$ -grams due to their sample complexity growing exponentially with  $n$  but can realistically encode lower-order  $n$ -grams in their weights and dynamically reweight different lags depending on the given prompt. To the best of our knowledge, this is the first in-context learning framework that explicitly couples an in-weight component (learning  $\pi^*$ ) with an in-context component (inferring  $\lambda$ ), providing a natural testbed for studying the fundamental in-weight / in-context dichotomy in LLMs.

## 2 DISENTANGLED TRANSFORMERS

The *disentangled transformer* (Friedman et al., 2023) is a modification of a standard Transformer with relative positional encodings (RPE) (Shaw et al., 2018), designed for enhanced interpretability by: (1) removing MLPs; (2) replacing residual connections with concatenation, creating an explicit residual stream that preserves computations from all previous layers; and (3) simplifying the attention mechanism to use a single attention matrix instead of query and key, and incorporates the value in the output matrix. Nichani et al. (2024) demonstrated that disentangled trans-

108 formers are equivalent to standard transformers using only attention layers. The model maps a  
 109 sequence of tokens  $s = (s_1, \dots, s_T)$  from a finite alphabet  $\mathcal{S}$  to a sequence of vectors. Each  
 110 token  $s_i$  is represented by its one-hot vector  $e_{s_i} \in \{0, 1\}^{|\mathcal{S}|}$ . This yields the initial representa-  
 111 tions  $\mathbf{H}^{(0)} = (e_{s_1}, \dots, e_{s_T}) \in \mathbb{R}^{d_0 \times T}$ , where  $d_0 = |\mathcal{S}|$ . The model consists of  $L$  layers. Let  
 112  $\mathbf{H}^{(l-1)} \in \mathbb{R}^{d_{l-1} \times T}$  be the input to layer  $l$ , where  $\mathbf{h}_i^{(l-1)}$  is its  $i$ -th column vector. For each head  
 113  $h \in \{1, \dots, H_l\}$ , the pre-softmax attention score  $e_{ij}^{(l,h)}$  from token  $i$  to  $j$  is computed as:  
 114

$$e_{ij}^{(l,h)} = (\mathbf{h}_i^{(l-1)})^\top \mathbf{W}_A^{(l,h)} \mathbf{h}_j^{(l-1)} + (\mathbf{h}_i^{(l-1)})^\top \mathbf{r}_{ij}^{(l,h)}. \quad (1)$$

115 Here,  $\mathbf{W}_A^{(l,h)} \in \mathbb{R}^{d_{l-1} \times d_{l-1}}$  is a learnable attention matrix and  $\mathbf{r}_{ij}^{(l,h)} = (\mathbf{R}_A^{(l,h)})_{i-j+1,:}$  is a relative  
 116 positional encoding vector retrieved from a learnable lookup table  $\mathbf{R}_A^{(l,h)} \in \mathbb{R}^{(T) \times d_{l-1}}$ . The attention  
 117 weights are computed via a causally masked softmax:  $\mathcal{A}_{ij}^{(l,h)} = [\text{softmax}(e_i^{(l,h)})]_j$ , where  $e_i^{(l,h)}$   
 118 is the vector of scores. The output of a single attention head is formed by concatenating the content  
 119 vector  $\mathbf{h}_j^{(l-1)}$  with a positional value embedding  $\mathbf{r}'_{ij}^{(l,h)}$  before the sum and it is then concatenated  
 120 with the input to form the layer output:  
 121

$$\hat{\mathbf{h}}_i^{(l,h)} = \sum_{j=1}^T \mathcal{A}_{ij}^{(l,h)} \text{Concat} \left( \mathbf{h}_j^{(l-1)}, \mathbf{r}'_{ij}^{(l,h)} \right) \quad \mathbf{H}^{(l)} = \text{Concat} \left( \mathbf{H}^{(l-1)}, \hat{\mathbf{H}}^{(l,1)}, \dots, \hat{\mathbf{H}}^{(l,H_l)} \right).$$

122 The positional value embeddings  $\mathbf{r}'_{ij}^{(l,h)}$  are retrieved from a second lookup table  $\mathbf{R}_V^{(l,h)} \in \mathbb{R}^{T \times d_R}$ ,  
 123 where  $d_R$  is a fixed hyperparameter. The dimension of the representation thus grows according  
 124 to the recurrence  $d_l = d_{l-1} + H_l \cdot (d_{l-1} + d_R)$ . After  $L$  layers, a final linear layer with matrix  
 125  $\mathbf{W}_O \in \mathbb{R}^{|\mathcal{S}| \times d_L}$  maps the final representation  $\mathbf{H}^{(L)}$  to logit predictions.  
 126

### 3 MIXTURE OF TRANSITION DISTRIBUTIONS FOR IN-CONTEXT LEARNING

131 The Mixture of Transition Distributions (MTD) model, introduced by Raftery (1985), is a higher-  
 132 order Markov chain that offers a parsimonious representation of long-range dependencies. The core  
 133 idea is to model the probability of the next state as a convex combination of several first-order  
 134 transition probabilities, each conditioned on a different past state (or lag).  
 135

136 **Model Definition:** Let  $\mathbf{Y} = (Y_1, \dots, Y_T)$  be a sequence of random variables tak-  
 137 ing values in a finite alphabet  $\mathcal{Y} = \{1, \dots, q\}$ . The MTD model of order  $m$  ex-  
 138 plains this sequence by positing a corresponding sequence of unobserved latent vari-  
 139 ables  $\mathbf{Z} = (Z_{m+1}, \dots, Z_T)$ , where each  $Z_t \in \{1, \dots, m\}$  acts as a switch, select-  
 140 ing which of the  $m$  previous tokens,  $Y_{t-1}, \dots, Y_{t-m}$ , will influence the current token  $Y_t$ .  
 141 The selection of this lag is a random event, governed by the mixture  
 142 weights  $\boldsymbol{\lambda} = (\lambda_1, \dots, \lambda_m)$  with  $\lambda_g \geq 0$  for all  $g$  and  $\sum_{g=1}^m \lambda_g = 1$ ,  
 143 such that the probability of choosing lag  $g$  is given by  $\mathbb{P}(Z_t = g) = \lambda_g$ .  
 144 Once the lag  $Z_t = g$  is sampled, the next token  $Y_t$  is generated from a  
 145 first-order transition that depends only on the state at the sampled position,  
 146  $Y_{t-g}$ . This is captured by a transition matrix  $\boldsymbol{\pi} \in \mathcal{P}$  with  $\mathcal{P}$  the  
 147 set of  $q \times q$  row-stochastic matrix defining the conditional probabilities  
 148  $\pi(i, j) = \mathbb{P}(Y_t = j \mid Y_{t-g} = i, Z_t = g)$ . By marginalizing over the  
 149 unobserved latent variable  $Z_t$ , we obtain the model's overall predictive  
 150 distribution:  
 151

152 **Definition 1** (Mixture Transition Distribution). *A sequence of random variables  $\mathbf{Y}$  follows an  $m$ -th  
 153 order MTD model if for all  $t > m$  and any history  $\mathbf{y}_1^{t-1}$ , the conditional probability of  $Y_t$  is:*

$$\mathbb{P}(Y_t = y_t \mid \mathbf{Y}_1^{t-1} = \mathbf{y}_1^{t-1}, \boldsymbol{\lambda}) = \sum_{g=1}^m \lambda_g \pi(y_{t-g}, y_t), \quad (2)$$

154 where the parameters  $\boldsymbol{\lambda} = (\lambda_1, \dots, \lambda_m)$  are the mixture weights and  $\boldsymbol{\pi}$  the transition matrix.  
 155

156 This structure allows to model different effective contexts, making it more flexible than a first-order  
 157 Markov chain preserving tractability by requiring only  $m - 1 + q(q - 1)$  parameters compared to  
 158 the  $q^m(q - 1)$  of a full  $m$ -th order Markov chain.  
 159

160 **The In-Context Learning Task:** We design an in-context learning task based on the MTD model  
 161 structured as follows: Given a transition matrix  $\boldsymbol{\pi}$  we generate sequences  $\mathbf{y}$ , by sampling for each a

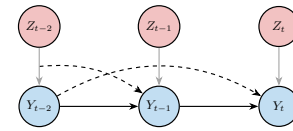


Figure 2: MTD for  $m=2$ .

new vector of mixture weights  $\lambda$  from a prior  $\lambda \sim \text{Dirichlet}(\alpha = 1)$ . This  $\lambda$  vector is the hidden task that defines the statistical structure of that particular sequence. The sequence  $\mathbf{y} = (y_1, \dots, y_T)$  is then generated according to the MTD model in equation 2. The learning objective for a model  $f \in \mathcal{F}$ , such as a transformer, is to predict the next token  $y_t$  given the context  $\mathbf{y}_1^{t-1}$ :

$$\inf_{f \in \mathcal{F}} \mathbb{E}_{\lambda \sim \text{Dirichlet}(\alpha)} \mathbb{E}_{\mathbf{y} \sim \text{MTD}(\lambda, \pi^*)} [\text{KL}(p(Y_t | \mathbf{y}_1^{t-1}, \lambda) \| f(\mathbf{y}_1^{t-1}))]. \quad (3)$$

To perform this prediction optimally, the model must effectively learn the mixture weights  $\lambda$  of the latent variables  $Z_t$ , which are not directly observable in the sequence and differ across sequences:

**In-Context Task:** Learn the unknown mixture weights  $\lambda$  given a single sequence  $\mathbf{y}$ .

**The Bayes Optimal Solution:** The solution to the ICL task (Eq. 3) is the Bayesian predictive distribution,  $p(Y_{t+1} | \mathbf{y}_1^t, \alpha)$ .

**Proposition 1** (Bayes-Optimal MTD Predictor). *Given the MTD model with a known transition matrix  $\pi$ , a prior  $p(\lambda | \alpha)$ , and an observed sequence  $\mathbf{y}_1^t$ , the Bayesian predictive distribution for  $Y_{t+1} = j$  is a convex combination of the lag-specific transition probabilities, weighted by the posterior mean of the mixture weights  $\lambda$ :*

$$p(Y_{t+1} = j | \mathbf{y}_1^t, \alpha) = \sum_{g=1}^m \hat{\lambda}_g^{\text{Bayes}} \cdot \pi(y_{t+1-g}, j) \quad \hat{\lambda}_g^{\text{Bayes}} := \mathbb{E}[\lambda_g | \mathbf{y}_1^t, \alpha] = \int_{\Delta_{m-1}} \lambda_g \cdot p(\lambda | \mathbf{y}_1^t, \alpha) d\lambda, \quad (4)$$

where  $p(\lambda | \mathbf{y}_1^t, \alpha) \propto p(\mathbf{y}_1^t | \lambda) p(\lambda | \alpha)$  is the posterior distribution with  $p(\mathbf{y}_1^t | \lambda) = \prod_{k=m+1}^t (\sum_{h=1}^m \lambda_h \pi(y_{k-h}, y_k))$  being the likelihood.

The derivation is provided in Appendix E. While elegant, the Bayes-optimal predictor is analytically intractable. The core issue is that the Dirichlet prior is not conjugate to the MTD likelihood, meaning the posterior distribution does not have a closed form. Consequently, the integral defining the posterior mean  $\hat{\lambda}_g^{\text{Bayes}}$  cannot be computed directly, necessitating the use of approximation methods.

**Mirror Descent (MD):** The intractability of the posterior mean motivates considering simpler point estimates, such as the Maximum Likelihood Estimate (MLE) or the Maximum A Posteriori (MAP) estimate which are equivalent under uniform Dirichlet prior. However, analytical computation of either the MLE or MAP is intractable necessitating iterative optimization methods. Methods such as Expectation–Maximization (EM) or Mirror Descent (MD) are preferred over standard gradient descent, as they are naturally adapted to the geometry of the simplex. For an extended discussion, see Appendix G. Furthermore, even if the MAP estimate could be found, it represents the mode of the posterior distribution, which does not coincide with the posterior mean in the Bayes-optimal predictor therefore leading to suboptimal predictions.

Mirror Descent, is a first-order method particularly well-suited for optimizing over the probability simplex  $\Delta_{m-1}$  Nemirovskij & Yudin (1983); Beck & Teboulle (2003). By using a Bregman divergence based on the negative entropy potential, MD results in the **Exponentiated Gradient (EG)** algorithm, which has a simple multiplicative update rule (see Appendix G.4 for details):

$$\lambda_g^{(k+1)} = \frac{\lambda_g^{(k)} \exp(\eta \cdot \nabla_{\lambda} \ell(\lambda^{(k)})_g)}{\sum_{h=1}^m \lambda_h^{(k)} \exp(\eta \cdot \nabla_{\lambda} \ell(\lambda^{(k)})_h)}, \quad (5)$$

where  $\eta > 0$  is the learning rate and  $\nabla_{\lambda} \ell(\lambda^{(k)})$  the gradient of the log-likelihood evaluated at  $\lambda^{(k)}$ . Instead of iterating the EG algorithm to convergence, we analyze a non-iterative estimator derived from a single update step, initialized at the center of the probability simplex ( $\lambda^{(0)} = (1/m, \dots, 1/m)$ ). This approach yields a computationally efficient, regularized approximation of the MLE, which we demonstrate serves as an effective proxy for the posterior mean.

**Proposition 2** (One-Step MD Estimator). *Initializing the EG algorithm (Eq. 5) at  $\lambda^{(0)} = (1/m, \dots, 1/m)$  and applying a single update step for the MTD model yields the estimator:*

$$\hat{\lambda}_g^{\text{MD}} := \frac{\exp\left(\eta \cdot m \sum_{k=m+1}^t \gamma_k(g)\right)}{\sum_{j=1}^m \exp\left(\eta \cdot m \sum_{k=m+1}^t \gamma_k(j)\right)} \quad \gamma_k(g) := p(Z_k = g | \mathbf{y}_1^k, \lambda^{(0)}) = \frac{\pi(y_{k-g}, y_k)}{\sum_{h=1}^m \pi(y_{k-h}, y_k)}, \quad (6)$$

where  $\gamma_k(g)$  is the posterior responsibility of lag  $g$  at step  $k > m$ , under the uniform prior.

The derivation is provided in Appendix G.4. This one-step estimator computes, for each step  $k$  in the sequence, the posterior probability that lag  $g$  was responsible for generating  $y_k$  (assuming all lags equally likely a priori). These responsibilities are summed across the sequence and fed into a softmax function to produce the estimate  $\hat{\lambda}^{\text{MD}}$  with the learning rate  $\eta$  controlling its sharpness.

## 4 TRANSFORMERS IMPLEMENT ONE-STEP OF MIRROR DESCENT

We present our main theoretical result: a constructive proof that the one-step MD estimator can be implemented by a Transformer. The crucial mechanism relies on relative position encodings to correctly route information, allowing the self-attention layer to compute the posterior responsibilities.

**Proposition 3** (Transformer Implementation of the One-Step MD Estimator). *Given an MTD model of order  $m$  with a known transition matrix  $\pi^* \in \mathcal{P}$ . For any sequence  $\mathbf{y}_{1:T}$  of length  $T \geq m$ , there exists a three-layer disentangled Transformer  $\tilde{\mathcal{T}}$  with single head,  $d_0 = q$  and  $d_R \geq m$  that implements the one-step MD estimator. The Transformer produces the predictive distribution for the next token  $Y_{t+1}$  at position  $t$  as:*

$$\tilde{\mathcal{T}}(\mathbf{y}_{1:T})_T = \sum_{g=1}^m \tilde{\lambda}_g(\mathbf{y}_{1:T}) \cdot \pi(y_{T+1-g}, :) \quad \tilde{\lambda}_g(\mathbf{y}_{1:T}) = \frac{\exp\left(\frac{\beta}{T-m} \sum_{i=m+1}^T \gamma_i(g)\right)}{\sum_{h=1}^m \exp\left(\frac{\beta}{T-m} \sum_{i=m+1}^T \gamma_i(h)\right)}, \quad (7)$$

with the weights  $\tilde{\lambda}(\mathbf{y}_{1:T})$  computed exactly as the one-step MD estimate and  $\beta$  is a learnable parameter corresponding to the scaled learning rate of the MD algorithm.

In the following we prove Proposition 3 by explicitly constructing a 3-layer disentangled Transformer that implements the one-step MD estimator. The first layer computes the posterior responsibilities  $\gamma_i(g)$ , the second layer computes the logits  $\sum_{i=m+1}^T \gamma_i(g)$ , and the third layer produces the final estimate vector  $\tilde{\lambda}(\mathbf{y}_{1:T})$  within its attention weights.

**Layer 1, Posterior Responsibilities:** The first layer uses the attention matrix  $\mathbf{W}_A^{(1)}$  to compute the posterior responsibilities and the relative positional encoding  $\mathbf{r}'_{ij}$  to store it in the residual stream:

$$\mathbf{W}_A^{(1)} = \log \pi^*, (\mathbf{R}_A^{(1)})_{k,:} = \begin{cases} +\delta_1 \cdot \mathbf{1}^\top & 2 \leq k \leq m+1 \\ -\delta_1 \cdot \mathbf{1}^\top & \text{otherwise} \end{cases}, (\mathbf{R}_V^{(1)})_{k,:} = \begin{cases} \mathbf{e}_{k-1}^\top & 2 \leq k \leq m+1 \\ \mathbf{0}^\top & \text{otherwise} \end{cases}$$

$$\mathbf{R}_A^{(1)\top} = \delta_1 \begin{pmatrix} 1 & 2 & \dots & m+1 & m+2 & \dots & T \\ -1 & 1 & \dots & 1 & -1 & \dots & -1 \\ -1 & 1 & \dots & 1 & -1 & \dots & -1 \\ \vdots & \vdots & \ddots & \vdots & \vdots & \ddots & \vdots \\ -1 & 1 & \dots & 1 & -1 & \dots & -1 \end{pmatrix} \quad \mathbf{R}_V^{(1)\top} = \begin{pmatrix} 1 & 2 & \dots & \dots & m+1 & m+2 & \dots & T \\ 0 & 1 & 0 & \dots & 0 & 0 & \dots & 0 \\ 0 & 0 & 1 & \dots & 0 & 0 & \dots & 0 \\ \vdots & \vdots & \ddots & \vdots & \vdots & \vdots & \ddots & \vdots \\ 0 & 0 & \dots & 0 & 1 & 0 & \dots & 0 \end{pmatrix}$$

where  $\log$  is applied element-wise,  $k = i - j + 1$  is the relative position between token  $i$  and  $j$  shifted by 1. The lookup table  $\mathbf{R}_A^{(1)}$  biases attention to focus only on the first  $m$  relative positions (the lags). The lookup table  $\mathbf{R}_V^{(1)}$  uses one-hot vectors  $\mathbf{e}_k$  to copy the computed attention weight for a specific lag into the corresponding dimension of the output vector, thereby storing the responsibilities for different lags in distinct positions. The attention score  $e_{ij}$  for this layer is computed as per Equation 1. Given that the input is one-hot encoded, i.e.,  $\mathbf{h}_i^{(0)} = \mathbf{e}_{y_i}$ , the score becomes:

$$e_{ij} = \mathbf{e}_{y_i}^\top (\log \pi^*) \mathbf{e}_{y_j} + \mathbf{e}_{y_i}^\top \mathbf{r}_{ij}^{(1)} = \log \pi^*(y_i, y_j) + \begin{cases} +\delta & \text{if } 1 \leq i - j \leq m \\ -\delta & \text{otherwise} \end{cases},$$

where we used that the RPE vector  $\mathbf{r}_{ij}$  is constant with respect to the token values  $y_i$ . For a large  $\delta_1$ , the softmax only attends to keys  $j$  such that their relative position  $k = i - j$  is within the range  $[1, m]$ . The causal attention weights  $\mathcal{A}_{ij}^{(1)}$  for  $j \leq i$  are given by:  $\mathcal{A}_{ij}^{(1)} = \frac{\exp(e_{ij})}{\sum_{j'=1}^i \exp(e_{ij'})} = \frac{\pi^*(y_i, y_j) \exp(\mathbf{e}_{y_i}^\top \mathbf{r}_{ij}^{(1)})}{\sum_{j'=1}^i \pi^*(y_i, y_{j'}) \exp(\mathbf{e}_{y_i}^\top \mathbf{r}_{ij'}^{(1)})}$ . In the limit  $\delta_1 \rightarrow \infty$ , the behavior of the softmax changes based on the

270 position  $i$ . For the first token ( $i = 1$ ), the only valid key is itself ( $j' = 1$ ), which means the attention  
 271 is entirely self-contained, resulting in  $\mathcal{A}_{11}^{(1)} = 1$ . For any subsequent token ( $i > 1$ ), the terms in the  
 272 denominator corresponding to lags  $k \in [1, m]$  are scaled by  $\exp(\delta_1)$ , while all other terms, including  
 273 the diagonal ( $k = 0$ ), are scaled by  $\exp(-\delta_1)$  and vanish. This yields the following limit for  $i > 1$ :  
 274

$$275 \quad \mathcal{A}_{ij}^{(1)} = \begin{cases} \frac{\pi^*(y_i, y_j)}{\sum_{k=1}^m \pi^*(y_i, y_{i-k})} & i - j \in [m] \\ 0 & \text{otherwise} \end{cases} \quad \mathcal{A}^{(1)} = \begin{pmatrix} 1 & 0 & 0 & 0 & 0 & 0 & \dots \\ * & 0 & 0 & 0 & 0 & 0 & \dots \\ * & * & 0 & 0 & 0 & 0 & \dots \\ \vdots & \vdots & \ddots & \vdots & \vdots & \vdots & \dots \\ 0 & \dots & \gamma_{T-1}(m) & \dots & \gamma_{T-1}(2) & \gamma_{T-1}(1) & 0 \\ 0 & \dots & 0 & \gamma_T(m) & \dots & \gamma_T(2) & \gamma_T(1) \end{pmatrix}$$

281 where  $\hat{m} = \min(i - 1, m)$ . For positions  $i > m$ , where the MTD model is defined, the attention  
 282 mechanism thus computes  $\mathcal{A}_{ij}^{(1)} = \gamma_i(i - j)$  for the active lags ( $1 \leq i - j \leq m$ ). This expression is  
 283 precisely the posterior responsibility  $\gamma_i(g)$  from Equation 6, where the lag is  $g = i - j$ . For earlier  
 284 steps ( $1 < i \leq m$ ), the attention mechanism computes the natural counterpart by normalizing over  
 285 the  $i - 1$  available lags. The resulting attention matrix  $\mathcal{A}^{(1)}$  has a specific banded lower-triangular  
 286 structure. The output of this layer,  $\hat{h}_i^{(1)}$ , is the attention-weighted sum over the concatenated value  
 287 vectors. Given that the attention weights  $\mathcal{A}_{ij}$  compute the posterior responsibilities  $\gamma_i(g)$  (for  $i >$   
 288  $m$ ), and  $\mathbf{R}_V^{(1)}$  embeds the lag  $g = i - j$  as a one-hot vector  $\mathbf{e}_g$ , the output for a position  $i > m$  is:  
 289

$$290 \quad \hat{h}_i^{(1)} = \sum_{j=1}^{i-1} \mathcal{A}_{ij} \text{Concat}(\mathbf{e}_{y_j}, \mathbf{r}'_{ij}^{(1)}) = \sum_{g=1}^m \gamma_i(g) \text{Concat}(\mathbf{e}_{y_{i-g}}, \mathbf{e}_g). \quad (8)$$

293 This output is a convex combination, weighted by the posterior responsibilities, of vectors that each  
 294 concatenate two pieces of information: the one-hot encoding of the token at a given lag ( $\mathbf{e}_{y_{i-g}}$ ) and  
 295 the one-hot encoding of  $\mathbf{e}_g$  of the lag itself ( $g$ ):  
 296

$$297 \quad \hat{h}_i^{(1)} = \underbrace{\gamma_i(m) \begin{pmatrix} \mathbf{e}_{y_{i-m}} \\ 0 \\ \vdots \\ 1 \end{pmatrix}}_{\text{Lag } m} + \dots + \underbrace{\gamma_i(2) \begin{pmatrix} \mathbf{e}_{y_{i-2}} \\ 0 \\ 1 \\ \vdots \end{pmatrix}}_{\text{Lag } 2} + \underbrace{\gamma_i(1) \begin{pmatrix} \mathbf{e}_{y_{i-1}} \\ 1 \\ 0 \\ \vdots \end{pmatrix}}_{\text{Lag } 1} = \begin{pmatrix} \sum_{g=1}^m \gamma_i(g) \mathbf{e}_{y_{i-g}} \\ \gamma_i(1) \\ \gamma_i(2) \\ \vdots \\ \gamma_i(m) \end{pmatrix}$$

303 In essence, the top part of  $\hat{h}_i^{(1)}$  contains a weighted sum of past tokens (which is not be used), while  
 304 its bottom part explicitly stores the vector of posterior responsibilities with the value  $\gamma_i(g)$  for lag  $g$   
 305 stored at the  $g$ -th position within this second block (i.e.,  $\gamma_i(1)$  is first, followed by  $\gamma_i(2)$ , etc.).  
 306

**Layer 2, Summing Responsibilities:** The second layer sums along the sequence the responsibility  
 307 vectors computed in Layer 1, for tokens at positions  $i > m$ . This is achieved by setting  
 308 the content-based attention to zero ( $\mathbf{W}_A^{(2)} = \mathbf{0}$ ) and the value-rpe matrix to zero ( $\mathbf{R}_V^{(2)} = \mathbf{0}$ ).  
 309 The mechanism relies on the content-position interaction  $(\hat{h}_i^{(1)})^\top \mathbf{r}_{ij}^{(2)}$ . Crucially, the input vector  
 310  $\mathbf{h}_i^{(1)} = \text{Concat}(\mathbf{e}_{y_i}, \hat{h}_i^{(1)})$  retains in the residual stream the one-hot embedding  $\mathbf{e}_{y_i}$  of the current  
 311 token in its first  $q$  dimensions. The RPE table  $\mathbf{R}_A^{(2)}$  is structured to interact only with this part of the  
 312 vector, turning the dot product into a fixed bias:  
 313

$$315 \quad \mathbf{W}_A^{(2)} = \mathbf{0}_{d_1 \times d_1}, \quad (\mathbf{R}_A^{(2)})_{k,:} = \begin{cases} \mathbf{0}_{1 \times d_1} & \text{if } 1 \leq k \leq T - m, \\ [-\delta_2 \cdot \mathbf{1}_{1 \times q}, \mathbf{0}_{1 \times (q+m)}] & \text{otherwise} \end{cases}, \quad \mathbf{R}_V^{(2)} = \mathbf{0}$$

317 The attention score for the final query at  $i = T$  therefore simplifies to:  
 318

$$319 \quad e_{Tj} = (\mathbf{h}_T^{(1)})^\top \mathbf{r}_{Tj}^{(2)} = \begin{cases} (\mathbf{h}_T^{(1)})^\top \begin{pmatrix} -\delta_2 \cdot \mathbf{1}_q \\ \mathbf{0}_{q+m} \end{pmatrix} = -\delta_2 \cdot (\mathbf{e}_{y_T}^\top \mathbf{1}_q) = -\delta_2 & \text{if } 1 \leq j \leq m \\ (\mathbf{h}_T^{(1)})^\top \mathbf{0}_{d_1} = 0 & \text{otherwise} \end{cases}$$

323 In the limit  $\delta_2 \rightarrow \infty$ , the softmax places uniform attention only on the keys where the score is not  
 324  $-\infty$ . This results in uniform attention weights  $\mathcal{A}_{Tj} = 1/(T - m)$  for  $j \in [m + 1, T]$ , and zero  
 325

otherwise. The layer's output for the final token is therefore the exact average of the desired vectors:

$$\hat{\mathbf{h}}_T^{(2)} = \sum_{j=1}^T \mathcal{A}_{Tj} \text{Concat}(\mathbf{h}_j^{(1)}, \mathbf{r}'_{Tj}) = \frac{1}{T-m} \sum_{j=m+1}^T \text{Concat}(\mathbf{h}_j^{(1)}, \mathbf{0}) = \frac{1}{T-m} \begin{pmatrix} \sum_{j=m+1}^T \left( \sum_{g=1}^m \gamma_j(g) \mathbf{e}_{y_{j-g}} \right) \\ \sum_{j=m+1}^T \gamma_j(1) \\ \sum_{j=m+1}^T \gamma_j(2) \\ \vdots \\ \sum_{j=m+1}^T \gamma_j(m) \\ \mathbf{0} \end{pmatrix}$$

Defining  $\boldsymbol{\Gamma}_j = (\gamma_j(1), \gamma_j(2), \dots, \gamma_j(m))^\top$ ; the  $m$ -dimensional sub-block  $\hat{\mathbf{h}}_{q+1:q+m}^{(2)} = \sum_j \boldsymbol{\Gamma}_j$  contains the average responsibility vectors,  $\frac{1}{T-m} \sum_{j=m+1}^T \boldsymbol{\Gamma}_j$ , which is exactly the quantity needed to implement the one-step MD estimator in Prop. 2.

**Layer 3, Final Predictive Weights:** The third and final layer uses the averaged responsibilities computed in Layer 2 to produce the final predictive weights,  $\tilde{\lambda}$ , which correspond to the one-step MD estimate from Prop. 2. This is accomplished by using the RPE table,  $\mathbf{R}_A^{(3)}$ , to perform a selective dot product. The query vector for the final token,  $\mathbf{h}_T^{(2)}$ , contains the vector of averaged responsibilities in its final  $m$  coordinates. The RPE vectors in  $\mathbf{R}_A^{(3)}$  are constructed as scaled one-hot vectors that align with this sub-block, effectively using the dot product to "read out" the corresponding averaged responsibility. Similarly to layer 2, to only have non-zero attention only at the positions corresponding to the  $m$  lags, we use the one-hot embedding of the current token  $\mathbf{e}_{y_i}$  from the residual stream  $\mathbf{h}_i^{(2)} = \text{Concat}(\mathbf{e}_{y_i}, \hat{\mathbf{h}}_i^{(1)}, \hat{\mathbf{h}}_i^{(2)})$  to add a fixed bias  $\delta_3$  which drives the softmax to zero in the limit. The content-based attention and value-rpe are again disabled:

$$\mathbf{W}_A^{(3)} = \mathbf{0}_{d_2 \times d_2}, \quad (\mathbf{R}_A^{(3)})_{k,:} = \begin{cases} \overbrace{[\delta_3 \cdot \mathbf{1}_q^\top, \mathbf{0}_{q+m}^\top, \mathbf{0}_q^\top, \beta \cdot \mathbf{e}_k^\top, \mathbf{0}_q^\top]}^{\text{on } \mathbf{h}^{(0)}}, \overbrace{[\mathbf{0}_{q+m}^\top, \mathbf{0}_q^\top, \mathbf{0}_m^\top, \mathbf{0}_q^\top]}^{\text{on } \hat{\mathbf{h}}_{1:q}^{(1)}}, \overbrace{[\mathbf{0}_q^\top]}^{\text{on } \hat{\mathbf{h}}_{q+m+1:d_2}^{(2)}} & \text{if } k \in [m] \\ \overbrace{[-\delta_3 \cdot \mathbf{1}_q^\top, \mathbf{0}_{q+m}^\top, \mathbf{0}_q^\top, \mathbf{0}_m^\top, \mathbf{0}_q^\top]}^{\text{on } \mathbf{h}^{(1)}} & \text{otherwise} \end{cases}$$

Here,  $\mathbf{e}_k$  is a one-hot vector in  $\mathbb{R}^{d_2}$  that selects the coordinate corresponding to the  $k$ -th responsibility in  $\mathbf{h}_T^{(2)}$ , and  $\beta$  is the learnable scaled learning rate. Visually, the RPE table  $\mathbf{R}_A^{(3)}$  is a sparse matrix of scaled one-hot vectors:

$$\mathbf{R}_A^{(3)\top} = \begin{matrix} \mathbf{h}^{(0)} & \begin{matrix} [1, \dots, m] \\ +\delta_3 \cdot \mathbf{1}_q, \dots, +\delta_3 \cdot \mathbf{1}_q \end{matrix} & \dots & \dots & T \\ \hat{\mathbf{h}}^{(1)} & \begin{matrix} \mathbf{0} \\ 0 \end{matrix} & \mathbf{0} & -\delta_3 \cdot \mathbf{1}_q & -\delta_3 \cdot \mathbf{1}_q \\ \boldsymbol{\Gamma} & \begin{matrix} \mathbf{0} \\ [\beta \mathbf{e}_1, \beta \mathbf{e}_2, \dots, \beta \mathbf{e}_m] \end{matrix} & \mathbf{0} & \mathbf{0} & \mathbf{0} \\ \hat{\mathbf{h}}_{q+m+1:d_2}^{(2)} & \mathbf{0} & \mathbf{0} & \mathbf{0} & \mathbf{0} \end{matrix}$$

Since  $\mathbf{W}_A^{(3)} = \mathbf{0}$ , the score simplifies to the content-position interaction  $(\mathbf{h}_T^{(2)})^\top \mathbf{r}_{Tj}^{(3)}$  and  $\mathbf{r}_{Tj}^{(3)}$  is constructed to be non-zero only for relative positions  $g = T-j+1 \in [1, m]$ . For these lags, the RPE is a scaled one-hot vector that acts as a selector, using the dot product to extract the corresponding averaged responsibility stored in  $\mathbf{h}_T^{(2)}$ :

$$e_{Tj} = (\mathbf{h}_T^{(2)})^\top \mathbf{r}_{Tj}^{(3)} = \begin{cases} (\mathbf{h}_T^{(0)})^\top (\delta_3 \mathbf{1}_q) + (\boldsymbol{\Gamma})_T^\top (\beta \mathbf{e}_g) & \text{if } g \in [m] \\ -\delta_3 \cdot (\mathbf{e}_{y_T}^\top \mathbf{1}_q) & \text{otherwise.} \end{cases}$$

The attention scores for the final token,  $e_{T,:}$ , becomes the scaled averaged responsibility:

$$\mathbf{e}_{T,:} = \left( -\delta_3, \dots, -\delta_3, \underbrace{+\delta_3 + \beta \frac{\sum_{i=m+1}^T \gamma_i(m)}{T-m}}_{\text{pos } T-m+1}, \dots, \underbrace{+\delta_3 + \beta \frac{\sum_{i=m+1}^T \gamma_i(2)}{T-m}}_{\text{pos } T-1}, \underbrace{+\delta_3 + \beta \frac{\sum_{i=m+1}^T \gamma_i(1)}{T-m}}_{\text{pos } T} \right)$$

After applying the softmax and in the limit of large  $\delta_3$ , the attention weights for the last token compute the MD estimate of the mixture weights  $\tilde{\lambda}_g$  and place them at the correct positions:

$$\lim_{\delta_3 \rightarrow \infty} \mathcal{A}_{T,T-g} = \frac{\exp\left(\beta \frac{\sum_{i=m+1}^T \gamma_i(g)}{T-m}\right)}{\sum_{k=1}^m \exp\left(\beta \frac{\sum_{i=m+1}^T \gamma_i(k)}{T-m}\right)} \quad \lim_{\delta_3 \rightarrow \infty} \mathcal{A}_{T,:} = \left( \dots, 0, \underbrace{\tilde{\lambda}_m}_{T-m+1}, \dots, \underbrace{\tilde{\lambda}_2}_{T-1}, \underbrace{\tilde{\lambda}_1}_T \right).$$

378 This final attention operation is the core of the estimation process. It computes the mixture weights  
 379  $\tilde{\lambda}$ , which serve as the in-context estimates of token importance, thus realizing the mechanism of  
 380 in-context learning this work seeks to understand.  
 381

382 **Output Layer:** The final step of the construction is to apply the output matrix  $\tilde{W}_O$  to the final hid-  
 383 den state  $\hat{h}_T^{(3)}$  to produce the predictive distribution over the next token. The matrix  $\tilde{W}_O$  learns the  
 384 known transition matrix  $\pi^*$  and selectively applies it to the embedding of the last token. The output  
 385 of the third attention layer,  $\hat{h}_T^{(3)}$ , is a weighted sum of the hidden states from the second layer, where  
 386 the weights are the estimated mixture weights  $\tilde{\lambda}_g$ :  $\hat{h}_T^{(3)} = \sum_{j=1}^T \mathcal{A}_{Tj}^{(3)} \hat{h}_j^{(2)} = \sum_{g=1}^m \tilde{\lambda}_g \hat{h}_{T-g}^{(2)}$ . The  
 387 first  $q$  components of any hidden state  $\hat{h}_j^{(k)}$ , due to the residual stream, simply contain the original  
 388 input  $\hat{h}_j^{(0)} = e_{y_j}$ . Consequently, the first  $q$  components of  $\hat{h}_T^{(3)}$  are a  $\tilde{\lambda}$ -weighted combination of the  
 389 one-hot embeddings of the relevant past tokens:  $(\hat{h}_T^{(3)})_{1:q} = \sum_{g=1}^m \tilde{\lambda}_g (\hat{h}_{T-g}^{(2)})_{1:q} = \sum_{g=1}^m \tilde{\lambda}_g e_{y_{T-g}}$ .  
 390 The full hidden stat is  $\hat{h}_T^{(3)} = \text{Concat}(\hat{h}_T^{(0)}, \hat{h}_T^{(1)}, \hat{h}_T^{(2)}, \hat{h}_T^{(3)})$  and the output matrix  $\tilde{W}_O \in \mathbb{R}^{q \times d_3}$   
 391 is structured to ignore all preceding blocks and operate only on the first  $q$  components of the final  
 392 block,  $\hat{h}_T^{(3)}$ . This is achieved by storing the transition matrix,  $\pi^{*\top}$ , in the corresponding sub-block:  
 393

$$\tilde{W}_O = \begin{pmatrix} \text{from } \hat{h}_T^{(0)} & \text{from } \hat{h}_T^{(1)} & \text{from } \hat{h}_T^{(2)} & \text{from } \hat{h}_T^{(3)} \\ \mathbf{0}_{q \times q} & \mathbf{0}_{q \times (q+m)} & \mathbf{0}_{q \times (2q+2m)} & [\pi^{*\top} \quad \mathbf{0}_{q \times (3q+4m)}] \end{pmatrix}.$$

394 Applying this matrix to the fully expanded final hidden state yields the predictive distribution:  
 395

$$\tilde{\mathcal{T}}(\mathbf{y}_{1:T})_T = [\pi^{*\top} \quad \mathbf{0}] \hat{h}_T^{(3)} = \pi^{*\top} (\hat{h}_T^{(3)})_{1:q} = \pi^{*\top} \left( \sum_{g=1}^m \tilde{\lambda}_g e_{y_{T-g}} \right) = \sum_{g=1}^m \tilde{\lambda}_g \pi^*(y_{T-g}, :).$$

400 This final vector is exactly the predictive distribution from Proposition 3, completing the proof.  
 401

## 402 5 WHY ONE-STEP MIRROR DESCENT WORKS

403 This section provides a theoretical analysis of the one-step MD estimator to formally justify its  
 404 success. We prove that a single MD update, initialized from a uniform prior, corresponds to an  
 405 estimator that is an approximation of the Bayesian posterior mean. Our results therefore, elucidate  
 406 the mechanism by which this simple, non-iterative procedure achieves good performance.  
 407

408 **One-Step MD as a First-Order Bayesian Approximation:** We establish a theoretical connec-  
 409 tion between the one-step Mirror Descent (MD) estimator and the Bayesian posterior mean. We  
 410 show that their first-order Taylor expansions around the state of no evidence coincide up to a scalar  
 411 constant. This result justifies interpreting the one-step MD estimator as a principled approxima-  
 412 tion to the Bayes-optimal predictor, especially in low-data regimes. The analysis hinges on treating  
 413 both estimators as functions of the log-likelihood gradient evaluated at the center of the simplex,  
 414  $\mathbf{g} := \nabla_{\lambda} \ell(\lambda^{(0)})$ , and expanding them around the point of no evidence,  $\mathbf{g} = \mathbf{0}$ .  
 415

416 **Theorem 1** (First-Order Equivalence of the Estimators). *Let  $\hat{\lambda}^{MD}(\mathbf{g}; \eta)$  be the one-step MD esti-  
 417 mator with learning rate  $\eta$ , and let  $\hat{\lambda}^{Bayes}(\mathbf{g})$  be the Bayesian posterior mean under the linearized  
 418 likelihood. The two estimators are first-order equivalent at  $\mathbf{g} = \mathbf{0}$  for  $\eta = \frac{1}{m+1}$ .*  
 419

420 **Learning-rate scaling via a Lipschitz (smoothness) constant:** We established a first-order equi-  
 421 valence between the one-step MD estimator and the Bayesian posterior mean at  $\mathbf{g} = \mathbf{0}$  (the “no-  
 422 evidence” regime). For a sequence of length  $T$ , however, the gradient norm  $|\mathbf{g}|$  scales with  $T$  see  
 423 App. J, raising the question of how to scale the learning rate of  $\hat{\lambda}^{MD} = \text{softmax}(\eta \mathbf{g})$  with  $T$ . Mirror  
 424 Descent theory suggests choosing the learning rate inversely proportional to the relative smoothness  
 425 constant  $L_{\text{rel}}$  (Bauschke et al., 2017). Because our MD update uses a negative entropy regularizer,  
 426 smoothness is defined w.r.t. the KL-divergence. Convergence requires  $\eta \leq 1/L_{\text{rel}}$ . We now bound  
 427 this constant and find exactly the scaling implemented in the Transformer in Prop. 3.  
 428

429 **Theorem 2** (Relative Smoothness and  $\eta$  scaling at the uniform mixture). *At the uniform vector  
 430  $\lambda = (1/m, \dots, 1/m)$ , the loss  $f(\lambda) = -\ell(\lambda)$  is  $L_{\text{rel}}$ -smooth relative to the KL-divergence, with*

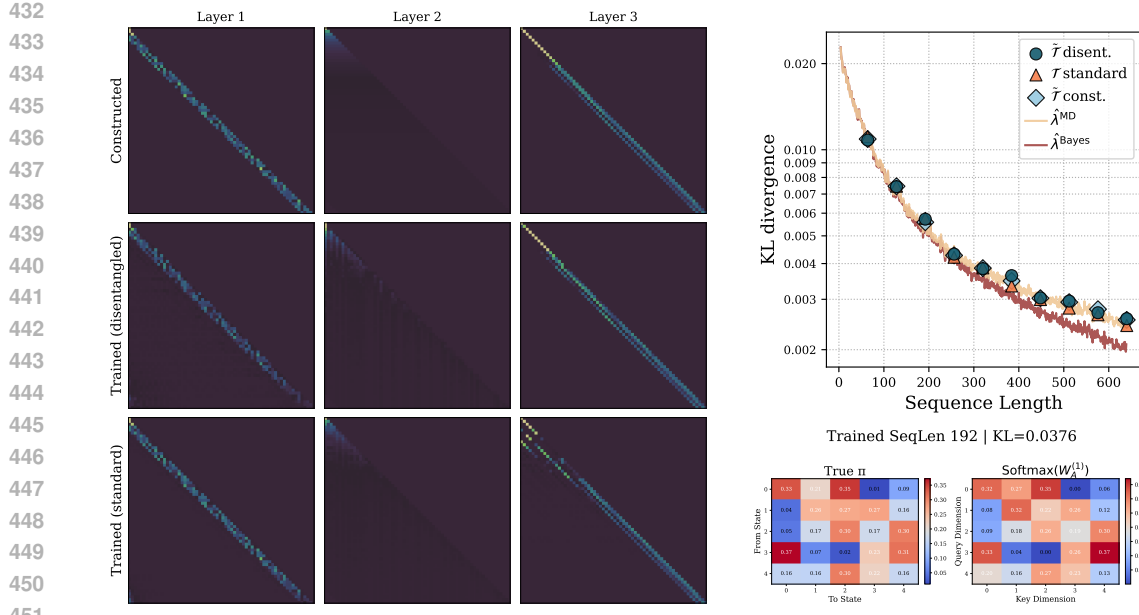


Figure 4: **Comparison of Trained and Constructed Transformers.** **Left:** Attention maps of the trained transformer (disentangled and standard) versus our theoretical construction (seq. length 64). **Right (top):** KL divergence to the ground truth transition probabilities for the trained transformers, the constructed transformer, and the one-step MD estimator across sequence lengths. **Right (bottom):** First-layer attention softmax  $Softmax(W_A^1)$  vs. true transitions matrix  $\pi^*$  for a trained model.

$L_{\text{rel}} \leq (T - m) m^2$ . Consequently, the stable MD step-size rule  $\eta \leq \frac{1}{L_{\text{rel}}}$  yields the asymptotic scaling  $\eta = \Theta\left(\frac{1}{T}\right)$  for fixed  $m$ .

**Beyond the Local Approximation, The Implicit Regularization of Mirror Descent:** The first-order equivalence in Theorem 3 holds only for short sequences, where the log-likelihood gradient is small. For longer sequences, neglected higher-order terms become significant, and the one-step estimator diverges from the Bayesian mean. Empirically, however, a few additional Mirror Descent substantially reduces this gap (see Figure 5). In this regime, iterating MD to convergence yields the suboptimal MLE, while early stopping provides a much closer match to the Bayesian mean. We propose that this effect arises from implicit regularization. Specifically, early-stopped MD approximately solves an entropy-regularized optimization problem of the form  $\min_{\lambda} -\ell(\lambda) + \gamma H(\lambda)$  with the iterates tracking the corresponding regularization path (Suggala et al., 2018). Along this path, performance on par with the Bayes-optimal estimator is achieved for an appropriate choice of regularization  $\gamma$  (see Figure. 3). Thus, early stopping is effectively equivalent to selecting this favorable point on the entropy-regularized path, avoiding the suboptimal MLE.

## 6 EXPERIMENTS

We report empirical validation of the main claims and additional experimental details in App.B as well as additional experiments in App.D.

**Setup:** We train 3-layer disentangled transformers  $\tilde{\mathcal{T}}_{\text{disent}}$  with single head with learned relative positional and one-hot semantic embeddings as well as 3-layer standard transformers  $\mathcal{T}_{\text{standard}}$  (no disentanglement) with single head attention with standard parameterization given by Query-Key-Value with learned relative positional and learned semantic embeddings. We sample a fixed  $q, m, \pi$

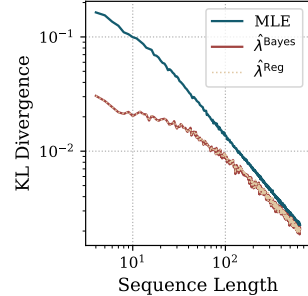


Figure 3: **Regularized Estimator.** Comparison with Bayes and MLE estimators.

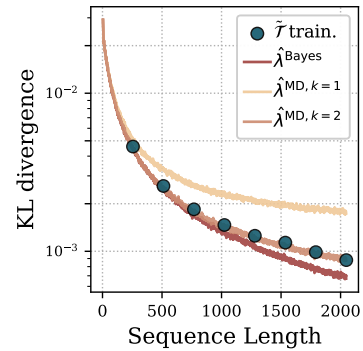
486 and at each iteration we sample a set of  $\{\lambda_i\}_{i=1}^B$  with  $B = 128$  the batch size and  $\lambda_i \sim \text{Dir}(\alpha)$  and  
 487 generate  $B$  sequences according to the MTD model. We train the model for  $10^6$  iterations using the  
 488 Adam optimizer and MSE loss over the last token in the sequence for various sequence lengths. The  
 489 learning rate is  $10^{-2}$  and decaying it at 0.5 and 0.75 of the iterations by a factor of 0.1.

490 **Results for one-step MD:** We plot the KL divergence with the ground truth transition probabilities  
 491 between the trained transformer  $\tilde{\mathcal{T}}_{\text{disent.}}$  and  $\mathcal{T}_{\text{standard.}}$  compared to our theoretical construction  $\tilde{\mathcal{T}}_{\text{constr.}}$ ,  
 492 the one-step MD estimator  $\hat{\lambda}^{\text{MD}}$  and the optimal-Bayes estimator  $\hat{\lambda}^{\text{Bayes}}$  (we compute it via MCMC  
 493 see App. F.1) for various sequence lengths in Figure 4 (right). We observe that both the disentangled  
 494 and standard trained transformers match the performance of the theoretical construction and the  
 495 one-step MD estimator: for small sequence lengths, the latter serves as a good proxy for the optimal  
 496 Bayes estimator, validating our theoretical result in Theorem 3, whereas for longer sequences it  
 497 becomes suboptimal. By inspecting the attention maps of the trained transformers (both standard  
 498 and disentangled) in Figure 4 (left) we can see that they actually learn to extract the responsibilities  
 499  $\gamma(g)_i$  as expected from our construction (for all three models, the locations of low and high attention  
 500 entries, and the diagonal structure induced by the MTD order, are closely aligned). To further  
 501 validate if the attention matrix in the first layer actually learns the ground truth transition matrix  $\pi^*$   
 502 we plot the heatmap of the first attention softmax  $\text{Softmax}(\mathbf{W}_1^A)$  vs.  $\pi^*$  as well compute the average  
 503 row-wise KL divergence between the two matrices Figure 4 (bottom-right) more results in App. D.  
 504 For both the  $\hat{\lambda}^{\text{MD}}$  and  $\tilde{\mathcal{T}}_{\text{constr.}}$  we tune the learning rate  $\beta$  and  $\eta$  via grid search to minimize the KL  
 505 divergence (see Section B.1 for more details).

506 **Results multi-step MD:** To further validate the hypothesis  
 507 that Transformers can learn to implement Mirror Descent to  
 508 solve the task, we plot the KL divergence for the 5-layer  
 509 trained transformer  $\tilde{\mathcal{T}}_{\text{train.}}$  compared to the multi-step MD  
 510 estimator  $\hat{\lambda}^{\text{MD}, k=i}$  where  $i$  is the number of steps for  
 511 various sequence lengths in Figure 5. We observe that the trained  
 512 transformers match the performance of 2-step of Mirror Descent.  
 513 Importantly, for longer sequences where the difference  
 514 between the 2-step MD and the Bayes-optimal solution be-  
 515 comes significant, the transformer still matches the 2-step per-  
 516 formance thus confirming that it is implementing an estimator  
 517 which matches at least in performance the 2-step MD. While  
 518 this evidence offers useful insights into how the transformer  
 519 behaves, it does not constitute direct evidence that it is im-  
 520 plementing multi-step MD. Extending our construction to the  
 521 multi-step MD setting is nontrivial and we leave this to future  
 522 work. Empirically, we find that a 5-layer transformer suffices  
 523 to match the performance of two steps, suggesting that the  
 524 responsibility computed from the first step might be reused to approximate the second.

## 525 7 CONCLUSIONS

526 This work identifies Mirror Descent as the core algorithm that transformers implement for in-context  
 527 learning of latent mixture weights. We introduced a novel framework using Mixture of Transition  
 528 Distribution (MTD) models to frame the inference of token importance as an in-context, latent variable  
 529 estimation task. Within this framework, we provided a constructive proof that a 3-layer trans-  
 530 former can exactly implement one-step of Mirror Descent, and we showed empirically that deeper  
 531 models learn to approximate multiple steps of the algorithm. Our theoretical analysis provides in-  
 532 sight into the one-step MD estimator, establishing its connection to the Bayes-optimal estimator and  
 533 deriving practical scaling laws for stable learning. Taken together, our findings extend the gradient-  
 534 based interpretation of ICL to sequential tasks over discrete domains, providing a new algorithmic  
 535 explanation for how transformers reason over latent structures.



536 **Figure 5: Multi-Step MD vs. 5-  
 537 Layer Transformer.** Comparison of  
 538 the KL divergence to the Bayesian pos-  
 539 terior mean.

## 540 REFERENCES

542 Kwangjun Ahn, Xiang Cheng, Hadi Daneshmand, and Suvrit Sra. Transformers learn to imple-  
 543 ment preconditioned gradient descent for in-context learning. *Advances in Neural Information*  
 544 *Processing Systems*, 2023.

545 Ekin Akyürek, Dale Schuurmans, Jacob Andreas, Tengyu Ma, and Denny Zhou. What learning  
 546 algorithm is in-context learning? investigations with linear models. In *The Eleventh International*  
 547 *Conference on Learning Representations*, 2022.

548 Adrian Raftery André Berchtold. The Mixture Transition Distribution Model for High-Order  
 549 Markov Chains and Non-Gaussian Time Series. *Statistical Science*, 17(3):328 – 356, 2002. doi:  
 550 10.1214/ss/1042727943.

552 Yu Bai, Fan Chen, Huan Wang, Caiming Xiong, and Song Mei. Transformers as statisticians:  
 553 Provable in-context learning with in-context algorithm selection. In *Thirty-seventh Conference on*  
 554 *Neural Information Processing Systems*, 2023a. URL <https://openreview.net/forum?id=liMSqUuVg9>.

556 Yu Bai, Fan Chen, Huan Wang, Caiming Xiong, and Song Mei. Transformers as statisticians:  
 557 Provable in-context learning with in-context algorithm selection. *Advances in neural information*  
 558 *processing systems*, 36, 2023b.

560 Heinz H Bauschke, Jérôme Bolte, and Marc Teboulle. A descent lemma beyond lipschitz gradient  
 561 continuity: first-order methods revisited and applications. *Mathematics of Operations Research*,  
 562 42(2):330–348, 2017.

563 Amir Beck and Marc Teboulle. Mirror descent and nonlinear projected subgradient methods for  
 564 convex optimization. *Operations Research Letters*, 31(3):167–175, 2003.

566 Alberto Bietti, Vivien Cabannes, Diane Bouchacourt, Herve Jegou, and Leon Bottou. Birth of a  
 567 transformer: A memory viewpoint. *Advances in Neural Information Processing Systems*, 2023a.

568 Alberto Bietti, Vivien Cabannes, Diane Bouchacourt, Herve Jegou, and Leon Bottou. Birth of a  
 569 transformer: A memory viewpoint. *Advances in Neural Information Processing Systems*, 36,  
 570 2023b.

572 Tom Brown, Benjamin Mann, Nick Ryder, Melanie Subbiah, Jared D Kaplan, Prafulla Dhariwal,  
 573 Arvind Neelakantan, Pranav Shyam, Girish Sastry, Amanda Askell, et al. Language models are  
 574 few-shot learners. *Advances in neural information processing systems*, 33:1877–1901, 2020.

575 Sébastien Bubeck, Varun Chandrasekaran, Ronen Eldan, Johannes Gehrke, Eric Horvitz, Ece Ka-  
 576 mar, Peter Lee, Yin Tat Lee, Yuanzhi Li, Scott Lundberg, et al. Sparks of artificial general  
 577 intelligence: Early experiments with gpt-4. *arXiv preprint arXiv:2303.12712*, 2023.

579 Stephanie Chan, Adam Santoro, Andrew Lampinen, Jane Wang, Aaditya Singh, Pierre Richemond,  
 580 James McClelland, and Felix Hill. Data distributional properties drive emergent in-context learn-  
 581 ing in transformers. *Advances in neural information processing systems*, 35:18878–18891, 2022.

582 Siyu Chen, Heejune Sheen, Tianhao Wang, and Zhuoran Yang. Unveiling induction heads: Prov-  
 583 able training dynamics and feature learning in transformers. In *The Thirty-eighth Annual Confer-  
 584 ence on Neural Information Processing Systems*, 2024. URL <https://openreview.net/forum?id=4fN2REs0Ma>.

586 Arthur Conmy, Augustine N. Mavor-Parker, Aengus Lynch, Stefan Heimersheim, and Adrià  
 587 Garriga-Alonso. Towards automated circuit discovery for mechanistic interpretability. In  
 588 *Thirty-seventh Conference on Neural Information Processing Systems*, 2023. URL <https://openreview.net/forum?id=89ia77nZ8u>.

591 Francesco D’Angelo, Francesco Croce, and Nicolas Flammarion. Selective induction heads:  
 592 How transformers select causal structures in context. In *The Thirteenth International Confer-  
 593 ence on Learning Representations*, 2025. URL <https://openreview.net/forum?id=bnJgZAQjWf>.

594 Ezra Edelman, Nikolaos Tsilivis, Benjamin Edelman, Eran Malach, and Surbhi Goel. The evolution  
 595 of statistical induction heads: In-context learning markov chains. *Advances in Neural Information  
 596 Processing Systems*, 37:64273–64311, 2024.

597

598 Nelson Elhage, Neel Nanda, Catherine Olsson, Tom Henighan, Nicholas Joseph, Ben Mann,  
 599 Amanda Askell, Yuntao Bai, Anna Chen, Tom Conerly, Nova DasSarma, Dawn Drain, Deep  
 600 Ganguli, Zac Hatfield-Dodds, Danny Hernandez, Andy Jones, Jackson Kernion, Liane Lovitt,  
 601 Kamal Ndousse, Dario Amodei, Tom Brown, Jack Clark, Jared Kaplan, Sam McCandlish, and  
 602 Chris Olah. A mathematical framework for transformer circuits. *Transformer Circuits Thread*,  
 603 2021.

604

605 Dan Friedman, Alexander Wettig, and Danqi Chen. Learning transformer programs. In *Thirty-  
 606 seventh Conference on Neural Information Processing Systems*, 2023. URL <https://openreview.net/forum?id=Pe9WxkN8Ff>.

607

608 Deqing Fu, Tianqi Chen, Robin Jia, and Vatsal Sharan. Transformers learn to achieve second-order  
 609 convergence rates for in-context linear regression. In *The Thirty-eighth Annual Conference on  
 610 Neural Information Processing Systems*, 2024. URL <https://openreview.net/forum?id=L8h6cozcbn>.

611

612 Shivam Garg, Dimitris Tsipras, Percy S Liang, and Gregory Valiant. What can transformers learn  
 613 in-context? a case study of simple function classes. *Advances in Neural Information Processing  
 614 Systems*, 35:30583–30598, 2022.

615

616 Jiachen Hu, Qinghua Liu, and Chi Jin. On limitation of transformer for learning hmms. *arXiv  
 617 preprint arXiv:2406.04089*, 2024.

618

619 M Emrullah Ildiz, Yixiao Huang, Yingcong Li, Ankit Singh Rawat, and Samet Oymak. From self-  
 620 attention to markov models: Unveiling the dynamics of generative transformers. *arXiv preprint  
 621 arXiv:2402.13512*, 2024.

622

623 Yuchen Li, Yuanzhi Li, and Andrej Risteski. How do transformers learn topic structure: Towards  
 624 a mechanistic understanding. In Andreas Krause, Emma Brunskill, Kyunghyun Cho, Barbara  
 625 Engelhardt, Sivan Sabato, and Jonathan Scarlett (eds.), *Proceedings of the 40th International  
 626 Conference on Machine Learning*, volume 202 of *Proceedings of Machine Learning Research*,  
 627 pp. 19689–19729. PMLR, 23–29 Jul 2023.

628

629 Arvind Mahankali, Tatsunori B Hashimoto, and Tengyu Ma. One step of gradient descent is provably  
 630 the optimal in-context learner with one layer of linear self-attention. In *The Twelfth International  
 631 Conference on Learning Representations*, 2024.

632

633 Ashok Vardhan Makkula, Marco Bondaschi, Adway Girish, Alliot Nagle, Martin Jaggi, Hyeji Kim,  
 634 and Michael Gastpar. Attention with markov: A framework for principled analysis of transformers  
 635 via markov chains. *arXiv preprint arXiv:2402.04161*, 2024.

636

637 Sewon Min, Xinxi Lyu, Ari Holtzman, Mikel Artetxe, Mike Lewis, Hannaneh Hajishirzi, and Luke  
 638 Zettlemoyer. Rethinking the role of demonstrations: What makes in-context learning work? In  
 639 Yoav Goldberg, Zornitsa Kozareva, and Yue Zhang (eds.), *Proceedings of the 2022 Conference  
 640 on Empirical Methods in Natural Language Processing*, pp. 11048–11064, Abu Dhabi, United  
 641 Arab Emirates, December 2022. Association for Computational Linguistics.

642

643 Arkadij Semenovič Nemirovskij and David Borisovich Yudin. Problem complexity and method  
 644 efficiency in optimization. 1983.

645

646 Timothy Nguyen. Understanding transformers via n-gram statistics. *arXiv preprint  
 647 arXiv:2407.12034*, 2024.

648

649 Eshaan Nichani, Alex Damian, and Jason D. Lee. How transformers learn causal structure with  
 650 gradient descent. In *Forty-first International Conference on Machine Learning*, 2024. URL  
 651 <https://openreview.net/forum?id=jNM4imlHZv>.

648 Catherine Olsson, Nelson Elhage, Neel Nanda, Nicholas Joseph, Nova DasSarma, Tom Henighan,  
 649 Ben Mann, Amanda Askell, Yuntao Bai, Anna Chen, Tom Conerly, Dawn Drain, Deep Ganguli,  
 650 Zac Hatfield-Dodds, Danny Hernandez, Scott Johnston, Andy Jones, Jackson Kernion, Liane  
 651 Lovitt, Kamal Ndousse, Dario Amodei, Tom Brown, Jack Clark, Jared Kaplan, Sam McCandlish,  
 652 and Chris Olah. In-context learning and induction heads. *Transformer Circuits Thread*, 2022.

653 Reese Pathak, Rajat Sen, Weihao Kong, and Abhimanyu Das. Transformers can optimally learn  
 654 regression mixture models. In *The Twelfth International Conference on Learning Representations*,  
 655 2024. URL <https://openreview.net/forum?id=sLkj91HIZU>.

656

657 Adrian E Raftery. A model for high-order markov chains. *Journal of the Royal Statistical Society  
 658 Series B: Statistical Methodology*, 47(3):528–539, 1985.

659

660 Nived Rajaraman, Marco Bondaschi, Kannan Ramchandran, Michael Gastpar, and Ashok Vard-  
 661 han Makkuvu. Transformers on markov data: Constant depth suffices. *arXiv preprint  
 662 arXiv:2407.17686*, 2024.

663 Allan Raventos, Mansheej Paul, Feng Chen, and Surya Ganguli. Pretraining task diversity and the  
 664 emergence of non-bayesian in-context learning for regression. In *Thirty-seventh Conference on  
 665 Neural Information Processing Systems*, 2023.

666 Michael Eli Sander, Raja Giryes, Taiji Suzuki, Mathieu Blondel, and Gabriel Peyré. How do trans-  
 667 formers perform in-context autoregressive learning ? In *Forty-first International Conference on  
 668 Machine Learning*, 2024. URL <https://openreview.net/forum?id=kZbTkpnafR>.

669

670 Adam Shai, Paul M. Riechers, Lucas Teixeira, Alexander Gietelink Oldenziel, and Sarah Marzen.  
 671 Transformers represent belief state geometry in their residual stream. In *The Thirty-eighth Annual  
 672 Conference on Neural Information Processing Systems*, 2024. URL <https://openreview.net/forum?id=YIB7REL8UC>.

673

674 Peter Shaw, Jakob Uszkoreit, and Ashish Vaswani. Self-attention with relative position representa-  
 675 tions. In *North American Chapter of the Association for Computational Linguistics*, 2018. URL  
 676 <https://api.semanticscholar.org/CorpusID:3725815>.

677

678 Aaditya K Singh, Ted Moskovitz, Felix Hill, Stephanie C. Y. Chan, and Andrew M Saxe. What needs  
 679 to go right for an induction head? a mechanistic study of in-context learning circuits and their  
 680 formation. In *Forty-first International Conference on Machine Learning*, 2024. URL <https://openreview.net/forum?id=O8rrX171D5>.

681

682 Arun Suggala, Adarsh Prasad, and Pradeep K Ravikumar. Connecting optimization and regulariza-  
 683 tion paths. *Advances in Neural Information Processing Systems*, 31, 2018.

684

685 Anej Sveté and Ryan Cotterell. Transformers can represent  $n$ -gram language models. *arXiv preprint  
 686 arXiv:2404.14994*, 2024.

687

688 Aditya Varre, Gizem Yüce, and Nicolas Flammarion. Learning in-context \$n\$-grams with trans-  
 689 formers: Sub-\$n\$-grams are near-stationary points. In *Forty-second International Conference on  
 690 Machine Learning*, 2025. URL <https://openreview.net/forum?id=OMwdvGDeHL>.

691

692 Johannes Von Oswald, Eyvind Niklasson, Ettore Randazzo, João Sacramento, Alexander Mordv-  
 693 intsev, Andrey Zhmoginov, and Max Vladymyrov. Transformers learn in-context by gradient  
 694 descent. In *International Conference on Machine Learning*, pp. 35151–35174. PMLR, 2023a.

695

696 Johannes Von Oswald, Eyvind Niklasson, Maximilian Schlegel, Sejjin Kobayashi, Nicolas Zucchet,  
 697 Nino Scherrer, Nolan Miller, Mark Sandler, Max Vladymyrov, Razvan Pascanu, et al. Uncovering  
 698 mesa-optimization algorithms in transformers. *arXiv preprint arXiv:2309.05858*, 2023b.

699

700 Sang Michael Xie, Aditi Raghunathan, Percy Liang, and Tengyu Ma. An explanation of in-context  
 701 learning as implicit bayesian inference. In *International Conference on Learning Representations*,  
 702 2022.

703 Steve Yadlowsky, Lyric Doshi, and Nilesh Tripuraneni. Pretraining data mixtures enable narrow  
 704 model selection capabilities in transformer models. *arXiv preprint arXiv:2311.00871*, 2023.

702 Oğuz Kaan Yüksel and Nicolas Flammarion. On the sample complexity of next-token prediction. In  
703 *The 28th International Conference on Artificial Intelligence and Statistics*, 2025. URL <https://openreview.net/forum?id=eJkNMwzZzy>.  
704

705 Ruiqi Zhang, Spencer Frei, and Peter L Bartlett. Trained transformers learn linear models in-context.  
706 *arXiv preprint arXiv:2306.09927*, 2023.  
707

708 Nicolas Zucchet, Francesco d’Angelo, Andrew K Lampinen, and Stephanie CY Chan. The emer-  
709 gence of sparse attention: impact of data distribution and benefits of repetition. *arXiv preprint*  
710 *arXiv:2505.17863*, 2025.  
711

712

713

714

715

716

717

718

719

720

721

722

723

724

725

726

727

728

729

730

731

732

733

734

735

736

737

738

739

740

741

742

743

744

745

746

747

748

749

750

751

752

753

754

755

756 **A NOTATION**  
757

758 Throughout this paper, we use non-bold letters for scalars (e.g.,  $\eta, \alpha$ ), lowercase bold letters for  
759 vectors (e.g.,  $\mathbf{h}, \boldsymbol{\lambda}$ ), and uppercase bold letters for matrices (e.g.,  $\mathbf{W}, \mathbf{H}, \boldsymbol{\pi}$ ). The  $i$ -th element of  
760 a vector  $\mathbf{v}$  is denoted by  $v_i$ , and the vector at position  $i$  in a sequence of vectors  $\mathbf{H}$  is written as  
761  $\mathbf{h}_i$ . The element in the  $i$ -th row and  $j$ -th column of a matrix  $\mathbf{A}$  is  $A_{ij}$ , and its  $i$ -th row vector is  
762  $\mathbf{A}_{i,:}$ . We use  $\mathbf{1}$  and  $\mathbf{0}$  to denote vectors or matrices of ones and zeros, respectively, with dimensions  
763 inferred from context. We use  $\mathbf{e}_k$  to denote a one-hot vector with a one at the  $k$ -th position; its  
764 dimensionality is specified or clear from context. The set of integers  $\{1, \dots, m\}$  is denoted by  $[m]$ .  
765 The probability simplex in  $\mathbb{R}^m$  is denoted by  $\Delta_{m-1}$ . The operator  $\text{Concat}(\cdot, \cdot)$  denotes the vertical  
766 concatenation of vectors or matrices. For vectors  $\mathbf{a} \in \mathbb{R}^{d_a}$  and  $\mathbf{b} \in \mathbb{R}^{d_b}$ , their concatenation results  
767 in a vector in  $\mathbb{R}^{d_a+d_b}$ . For matrices  $\mathbf{A} \in \mathbb{R}^{d_A \times T}$  and  $\mathbf{B} \in \mathbb{R}^{d_B \times T}$  with the same number of columns,  
768  $\text{Concat}(\mathbf{A}, \mathbf{B})$  is the block matrix  $\begin{pmatrix} \mathbf{A} \\ \mathbf{B} \end{pmatrix} \in \mathbb{R}^{(d_A+d_B) \times T}$ . Superscripts in parentheses, such as  $\mathbf{H}^{(l)}$ ,  
769 are used to index the layers of the Transformer. In the context of Transformer relative positional  
770 encodings, we use 1-based indexing for token positions  $i, j \in [T]$ . The relative position is mapped  
771 to a lookup table index  $k = i - j + 1$ . The approximations will be expressed using Landau notation,  
772 where a vector function  $\mathbf{f}(\mathbf{g}) = O(\|\mathbf{g}\|^p)$  signifies that  $\|\mathbf{f}(\mathbf{g})\| \leq C\|\mathbf{g}\|^p$  for some constant  $C$  in a  
773 neighborhood of  $\mathbf{g} = \mathbf{0}$ .  
774

775 **A.1 DIMENSIONALITY OF THE TRANSFORMER CONSTRUCTION**  
776

777 The disentangled Transformer architecture results in a hidden state that grows with each layer. The  
778 following table provides a summary of the dimensions at each stage of the construction. Note that  
779 the input to layer  $l$  is  $\mathbf{h}^{(l-1)}$ , and its output is  $\mathbf{h}^{(l)}$ , which is formed by concatenating the input with  
780 the result of the attention mechanism,  $\hat{\mathbf{h}}^{(l)}$ . We use  $q$  for the alphabet size and  $m$  for the MTD model  
781 order. For this construction, the RPE value dimension  $d_R$  is set to  $m$ .  
782

783 Table 1: Dimensionality of Hidden States in the Disentangled Transformer  
784

Layer	Description	Attention Output $\hat{\mathbf{h}}^{(l)}$	Concatenated Hidden State $\mathbf{h}^{(l)}$
0 (Input)	Token Embeddings	—	$\mathbf{h}^{(0)} \in \mathbb{R}^q$
1	Responsibilities	$\hat{\mathbf{h}}^{(1)} \in \mathbb{R}^{q+m}$	$\mathbf{h}^{(1)} = \text{Concat}(\mathbf{h}^{(0)}, \hat{\mathbf{h}}^{(1)}) \in \mathbb{R}^{2q+m}$
2	Summation	$\hat{\mathbf{h}}^{(2)} \in \mathbb{R}^{2q+m}$	$\mathbf{h}^{(2)} = \text{Concat}(\mathbf{h}^{(1)}, \hat{\mathbf{h}}^{(2)}) \in \mathbb{R}^{4q+2m}$
3	Weighting	$\hat{\mathbf{h}}^{(3)} \in \mathbb{R}^{4q+2m}$	$\mathbf{h}^{(3)} = \text{Concat}(\mathbf{h}^{(2)}, \hat{\mathbf{h}}^{(3)}) \in \mathbb{R}^{8q+4m}$
<b>Final Output Matrix</b>		$\widetilde{\mathbf{W}}_O \in \mathbb{R}^{q \times (8q+4m)}$	

794 **B EXPERIMENTAL DETAILS**  
795

796 This section provides additional details on the experimental setup, including the hyperparameter  
797 settings for all models and estimators used in our empirical validation.  
798

800 **B.1 HYPERPARAMETER TUNING**  
801

802 For the one-step Mirror Descent estimator ( $\hat{\lambda}^{\text{MD}}$ ) and our theoretical Transformer construction  
803 ( $\tilde{\mathcal{T}}_{\text{constr.}}$ ), the learning rate parameters  $\eta$  and  $\beta$  were not fixed but were tuned to optimize performance.  
804 For each sequence length evaluated, we performed a grid search over a range of potential  
805 values for  $\eta$  and  $\beta$ . The value that minimized the KL divergence to the true Bayesian posterior mean  
806 was selected for the final comparison plots. This ensures that both methods were evaluated under  
807 their optimal conditions.  
808

809 **B.2 PARAMETER SUMMARY**  
810

811 The following table summarizes the key parameters used in our experiments.  
812

810

811

Table 2: Summary of Experimental Parameters

812

813

Component	Parameter	Value
<b>Data Generation</b>		
	MTD model order ( $m$ )	3,4,5
	Vocabulary size ( $q$ )	5
	Sequence Length ( $T$ )	Varied (64 to 1984)
	Dirichlet Prior ( $\alpha$ )	Uniform ( $\alpha_g = 1$ for all $g$ )
	Transition Matrix ( $\pi$ )	Rows from Dirichlet ( $\alpha = 1$ )
<b>Mirror Descent (MD) Estimator</b>		
	Learning Rate ( $\eta$ )	Log grid: $[10^{-5}, 10^{-1}]$ , 1000 points
<b>Constructed Transformer (<math>\tilde{\mathcal{T}}_{\text{constr.}}</math>)</b>		
	Large Constant ( $\delta_1, \delta_2, \delta_3$ )	[100,100,100]
	Scaled Learning Rate ( $\beta$ )	Log grid: $[10^{-5}, 10^{-1}]$ , 1000 points
<b>Trained Transformer (<math>\tilde{\mathcal{T}}_{\text{disent.}}</math>)</b>		
	Architecture	3-layer & 5-layer Disentangled Transformer
	Attention Heads	1
	Concatenation	True
	Semantic Embeddings	one-hot
	Relative Positional Encodings	Learned
	RPE value dimension	$m$
	Embedding Dimension	$q$
	QK parametrization	False
	Value matrix	False
	Head output projection matrix	False
	Optimizer	Adam
	Learning Rate	$1 \times 10^{-3}$
	LR Schedule	Decay by 0.1 at 50% and 75% of training
	Batch Size	128
	Training Iterations	$1 \times 10^6$
	Loss Function	MSE on the last token prediction
<b>Trained Transformer (<math>\mathcal{T}_{\text{standard.}}</math>)</b>		
	Architecture	3-layer Standard Transformer
	Attention Heads	1
	Concatenation	False
	Semantic Embeddings	Learned
	Relative Positional Encodings	Learned
	Embedding Dimension	32
	QK parametrization	True
	Value matrix	True
	Head output projection matrix	True
	Optimizer	Adam
	Learning Rate	$1 \times 10^{-3}$
	LR Schedule	Decay by 0.1 at 50% and 75% of training
	Batch Size	128
	Training Iterations	$5 \times 10^5$
	Loss Function	MSE on the last token prediction
<b>MCMC for Bayes Estimator</b>		
	Sampler	Gibbs Sampling
	Burn-in Iterations	[200]
	Number of Samples (K)	[2000]

864  
865  
866  
867 **C RELATED WORKS**  
868  
869  
870  
871  
872  
873  
874  
875  
876  
877  
878

**Induction heads and interpretability** The emergence of ICL, as well as the more general ability of transformers to implement algorithms, has been linked to the formation of interpretable computational circuits Elhage et al. (2021) such as induction heads (Olsson et al., 2022), which are woven into sparse attention patterns (Zucchet et al., 2025). The development of these circuits is not monolithic; rather, they emerge in phases through the interaction of simpler subcircuits. Singh et al. (2024), for instance, use a causal framework to identify the key subcircuits whose interplay leads to the sudden formation of induction heads during training. This emergence itself also critically depends on the training data; specific distributional properties, such as burstiness and class imbalance, have been shown to be key drivers of this capability Chan et al. (2022); Zucchet et al. (2025). While much of this understanding comes from reverse-engineering circuits in pretrained models Conmy et al. (2023), a parallel line of research aims to create transformers that are interpretable by design, for example by training models that can be directly decompiled into human-readable programs Friedman et al. (2023).

**In-Context learning and gradient descent** Following initial empirical observations of ICL in transformers (Brown et al., 2020), a significant line of research has sought to understand its underlying mechanisms. Early work demonstrated that transformers can learn simple function classes like linear models in-context (Garg et al., 2022). This led to the hypothesis that transformer layers effectively implement optimization algorithms, with several studies showing they can perform computations analogous to gradient descent for in-context linear regression (Akyürek et al., 2022; Bai et al., 2023b; Von Oswald et al., 2023a;b). This gradient-based view has been extended to higher-order algorithms (Ahn et al., 2023; Fu et al., 2024) and given theoretical grounding, with proofs that gradient flow converges to a transformer that has learned the in-context task (Zhang et al., 2023). From a statistical learning perspective, this process has been formalized as "algorithm learning", where generalization is guaranteed by the algorithmic stability of the learned procedure (Li et al., 2023). Crucially, the emergence of this behavior is not guaranteed; it depends on sufficient pretraining task diversity (Raventos et al., 2023). This algorithmic paradigm also extends to linear autoregressive processes, where transformers have been shown to implement a gradient descent step to learn the transition matrix in-context (Sander et al., 2024).

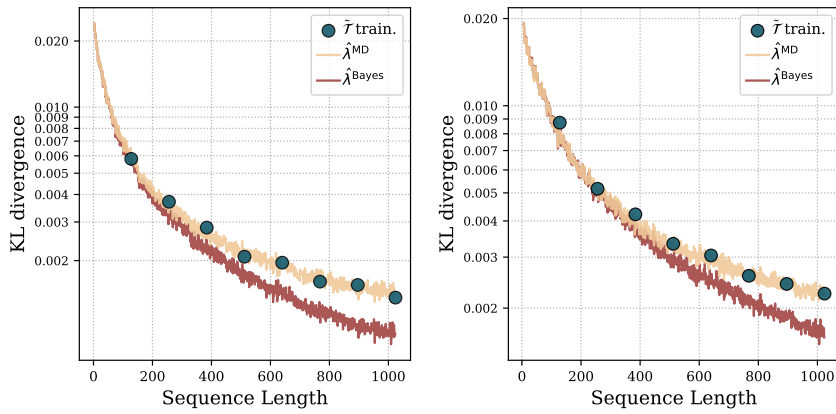
**In-Context learning, Markov chains and n-gram models** Our work is closely related to the literature analyzing ICL for sequential probabilistic models like n-grams and Markov chains. Foundational work by Yüksel & Flammarion (2025) established formal generalization bounds for next-token prediction on Markovian data, analyzing its sample complexity. Regarding transformers, several mechanistic studies have investigated how they implement learning algorithms for these models. For bigrams, transformers have been shown to develop induction heads that function like associative memories (Bietti et al., 2023b) and accurately compute posterior probabilities from statistical cues (Edelman et al., 2024). For first order Markov chains, Nichani et al. (2024) demonstrated that transformers learn the causal structure with gradient descent and implement induction heads to estimate the transition probabilities in-context, effectively implementing a Bayes-optimal estimator. This analysis was later extended to higher-order chains (Chen et al., 2024), while the work of D'Angelo et al. (2025) shows that transformers can even learn to select the correct Markov causal structure at inference time. Further theoretical results have explored the transformer loss landscape in this setting (Makkuvu et al., 2024), characterized in-context n-grams as near-stationary points (Varre et al., 2025), and shown that constant-depth transformers are sufficient to learn k-th order Markov chains (Rajaraman et al., 2024).

**Transformers and sequential models** Beyond specific learning algorithms, a broader line of work has explored the fundamental capabilities and limitations of transformers as sequential models. In terms of representational power, transformers with sparse attention have been shown to be capable of exactly representing any n-gram model (Svete & Cotterell, 2024). However, this expressive power has limits; for instance, transformers may be less effective at learning certain Hidden Markov Models (HMMs) compared to RNNs (Hu et al., 2024). Interestingly, when investigating the internal representations that enable inference in HMMs, Shai et al. (2024) showed that transformers maintain interpretable belief states that are linearly encoded in the residual stream. A strength of transformers is their ability to perform in-context model selection. It has been demonstrated that a single transformer can adaptively choose between different base algorithms or even qualitatively different tasks (e.g., regression vs. classification) based on the prompt (Bai et al., 2023a), effectively

918 selecting between different function classes in-context (Yadlowsky et al., 2023). While high-level  
 919 n-gram statistics can approximate transformer predictions, the mechanism for how the correct "rule"  
 920 is selected in-context remains an open question (Nguyen, 2024).

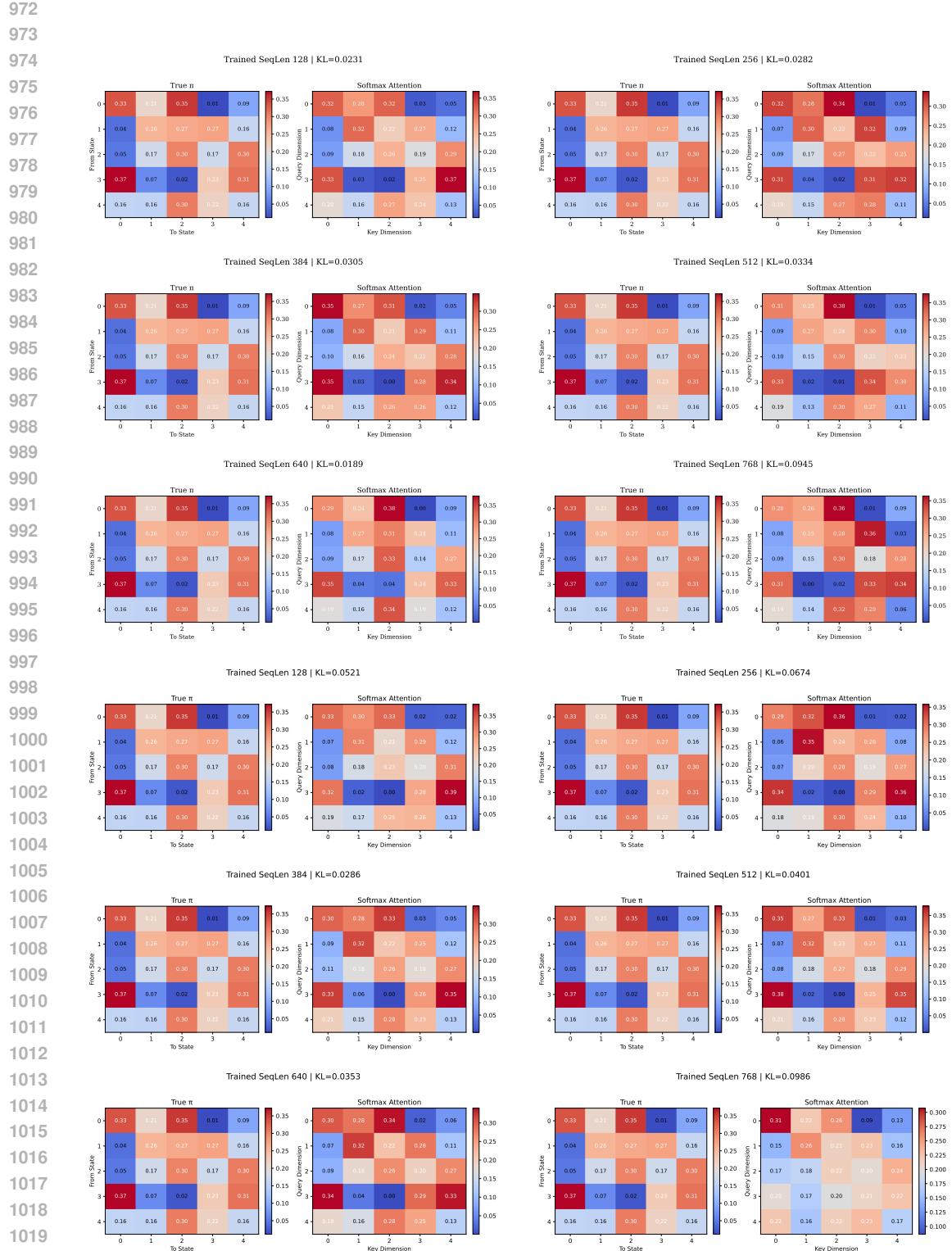
## 922 D ADDITIONAL EXPERIMENTS

923  
 924 In this section we repeat the main-text experiments for different MTD orders, comparing the trained  
 925 and constructed transformers: in addition to the  $m = 4$  case in the main text, we report results  
 926 for  $m = 3$  and  $m = 5$ . In Figure 6, we plot the KL divergence to the ground-truth transition  
 927 probabilities across sequence lengths for the trained transformers, the constructed transformer, and  
 928 the one-step MD estimator (orders 3 and 5). In Figure 7, we instead compare the learned first-layer  
 929 attention (softmax) to the true transition matrices for orders 3 and 5, with the average row-wise KL  
 930 divergence reported directly in each panel. Finally, Figure 8 reports attention grids for the trained  
 931 and constructed transformers (disentangled) at sequence length 64 for MTD orders  $m = 3$  and  
 932  $m = 5$ , analogous to the attention maps shown in Figure 4 (left) in the main text.



948 **Figure 6: KL divergence to the ground-truth** We report the KL divergence to the ground truth transition  
 949 probabilities for the trained transformers, the constructed transformer, and the one-step MD estimator across  
 950 sequence lengths **Left:** order 3 **Right:** order 5.

951  
 952  
 953  
 954  
 955  
 956  
 957  
 958  
 959  
 960  
 961  
 962  
 963  
 964  
 965  
 966  
 967  
 968  
 969  
 970  
 971





1080 **E DERIVATION OF THE BAYES-OPTIMAL MTD PREDICTOR**  
 1081

1082 Here, we provide the full derivation for the Bayes-optimal predictive distribution stated in Proposition  
 1083 1.

1084 Our goal is to derive the predictive distribution for the next state,  $p(Y_{t+1} | \mathbf{y}_1^t, \boldsymbol{\alpha})$ , given an observed  
 1085 data prefix  $\mathbf{y}_1^t = (y_1, \dots, y_t)$ . The unknown mixture weights  $\boldsymbol{\lambda} = (\lambda_1, \dots, \lambda_m)$  are assumed to be  
 1086 drawn from a Dirichlet prior distribution:

1087

$$p(\boldsymbol{\lambda} | \boldsymbol{\alpha}) = \text{Dirichlet}(\boldsymbol{\lambda} | \boldsymbol{\alpha}) = \frac{\Gamma(\sum_{g=1}^m \alpha_g)}{\prod_{g=1}^m \Gamma(\alpha_g)} \prod_{g=1}^m \lambda_g^{\alpha_g - 1}.$$

1091 The likelihood of the observed data given the parameters  $\boldsymbol{\lambda}$  is defined by the MTD model:  
 1092

1093

$$p(\mathbf{y}_1^t | \boldsymbol{\lambda}) = \prod_{k=m+1}^t p(y_k | \mathbf{y}_1^{k-1}, \boldsymbol{\lambda}) = \prod_{k=m+1}^t \left( \sum_{h=1}^m \lambda_h \pi(y_{k-h}, y_k) \right).$$

1096 Combining the likelihood and prior via Bayes' theorem yields the posterior distribution over the  
 1097 mixture weights:

1098

$$p(\boldsymbol{\lambda} | \mathbf{y}_1^t, \boldsymbol{\alpha}) \propto p(\mathbf{y}_1^t | \boldsymbol{\lambda}) \cdot p(\boldsymbol{\lambda} | \boldsymbol{\alpha}).$$

1100 The Bayesian predictive distribution is formulated by marginalizing the single-step prediction  
 1101  $p(Y_{t+1} = j | \mathbf{y}_1^t, \boldsymbol{\lambda})$  over this posterior distribution of  $\boldsymbol{\lambda}$ :

1102

$$p(Y_{t+1} = j | \mathbf{y}_1^t, \boldsymbol{\alpha}) = \int_{\Delta_{m-1}} p(Y_{t+1} = j | \mathbf{y}_1^t, \boldsymbol{\lambda}) \cdot p(\boldsymbol{\lambda} | \mathbf{y}_1^t, \boldsymbol{\alpha}) d\boldsymbol{\lambda},$$

1105 where  $\mathcal{S}$  is the probability simplex. The single-step prediction is simply the MTD model definition:

1106

$$p(Y_{t+1} = j | \mathbf{y}_1^t, \boldsymbol{\lambda}) = \sum_{g=1}^m \lambda_g \pi(y_{t+1-g}, j).$$

1109 Substituting this into the integral gives:  
 1110

1111

$$p(Y_{t+1} = j | \mathbf{y}_1^t, \boldsymbol{\alpha}) = \int_{\Delta_{m-1}} \left( \sum_{g=1}^m \lambda_g \pi(y_{t+1-g}, j) \right) p(\boldsymbol{\lambda} | \mathbf{y}_1^t, \boldsymbol{\alpha}) d\boldsymbol{\lambda}.$$

1114 By the linearity of expectation (and integration), the integral and the finite sum can be interchanged:  
 1115

1116

$$p(Y_{t+1} = j | \mathbf{y}_1^t, \boldsymbol{\alpha}) = \sum_{g=1}^m \pi(y_{t+1-g}, j) \left( \int_{\Delta_{m-1}} \lambda_g \cdot p(\boldsymbol{\lambda} | \mathbf{y}_1^t, \boldsymbol{\alpha}) d\boldsymbol{\lambda} \right).$$

1119 We recognize the term in the parentheses as the definition of the posterior mean of the parameter  $\lambda_g$ :  
 1120

1121

$$\hat{\lambda}_g^{\text{Bayes}} := \mathbb{E}[\lambda_g | \mathbf{y}_1^t, \boldsymbol{\alpha}] = \int_{\Delta_{m-1}} \lambda_g \cdot p(\boldsymbol{\lambda} | \mathbf{y}_1^t, \boldsymbol{\alpha}) d\boldsymbol{\lambda}.$$

1124 This substitution yields the final form of the Bayes-optimal predictor, completing the proof:  
 1125

1126

$$p(Y_{t+1} = j | \mathbf{y}_1^t, \boldsymbol{\alpha}) = \sum_{g=1}^m \hat{\lambda}_g^{\text{Bayes}} \cdot \pi(y_{t+1-g}, j).$$

1128 **E.1 THE STRUCTURE OF THE BAYES-OPTIMAL ESTIMATOR**

1131 While the posterior mean is intractable to compute, its structure can be derived exactly. In particular  
 1132 it can be shown that the MTD posterior is a finite mixture of Dirichlet distributions, and from this, we  
 1133 can derive that the mean of the posterior preserves the classic 'add-constant' structure of conjugate  
 Bayesian models, where the unobserved data counts are replaced by their posterior expectation.

1134  
 1135 **Proposition 4** (Posterior as a Mixture of Dirichlets). *Given the MTD likelihood  $L(\boldsymbol{\lambda}) = p(\mathbf{y}_1^t \mid \boldsymbol{\lambda})$  and a Dirichlet prior  $p(\boldsymbol{\lambda} \mid \boldsymbol{\alpha}) = \text{Dir}(\boldsymbol{\lambda} \mid \boldsymbol{\alpha})$ , the posterior distribution is a finite mixture of*  
 1136 *Dirichlet distributions:*

1137  
 1138 
$$p(\boldsymbol{\lambda} \mid \mathbf{y}_1^t, \boldsymbol{\alpha}) = \sum_{z \in \{1, \dots, m\}^{t-m}} \pi(z) \cdot \text{Dir}(\boldsymbol{\lambda} \mid \boldsymbol{\alpha} + k(z)), \quad (9)$$
  
 1139

1140 where  $z = (z_{m+1}, \dots, z_t)$  is a latent assignment path,  $k(z)$  is the vector of counts of each lag in  
 1141 path  $z$ , and  $\pi(z) = p(Z = z \mid \mathbf{y}_1^t, \boldsymbol{\alpha})$  are the true posterior probabilities of the latent paths.  
 1142

1143 *Proof.* We begin with Bayes' theorem for the posterior distribution:

1144  
 1145 
$$p(\boldsymbol{\lambda} \mid \mathbf{y}_1^t, \boldsymbol{\alpha}) \propto p(\mathbf{y}_1^t \mid \boldsymbol{\lambda}) \cdot p(\boldsymbol{\lambda} \mid \boldsymbol{\alpha}).$$

1146 The central idea is to express the observed-data likelihood,  $p(\mathbf{y}_1^t \mid \boldsymbol{\lambda})$ , by marginalizing over all  
 1147 possible latent assignment paths  $z$ . A path  $z = (z_{m+1}, \dots, z_t)$  specifies which lag was used at each  
 1148 step  $k$ .

1149  
 1150 
$$p(\mathbf{y}_1^t \mid \boldsymbol{\lambda}) = \sum_{z \in \{1, \dots, m\}^{t-m}} p(\mathbf{y}_1^t, z \mid \boldsymbol{\lambda}).$$

1151 The joint probability of the data and a specific path  $z$ , known as the complete-data likelihood, is  
 1152 given by:

1153  
 1154 
$$\begin{aligned} p(\mathbf{y}_1^t, z \mid \boldsymbol{\lambda}) &= \prod_{k=m+1}^t p(y_k, z_k \mid \mathbf{y}_1^{k-1}, \boldsymbol{\lambda}) \\ 1155 &= \prod_{k=m+1}^t p(z_k \mid \boldsymbol{\lambda}) \cdot p(y_k \mid \mathbf{y}_1^{k-1}, z_k, \boldsymbol{\lambda}) \\ 1156 &= \prod_{k=m+1}^t \lambda_{z_k} \cdot \pi(y_{k-z_k}, y_k). \end{aligned}$$
  
 1157  
 1158  
 1159  
 1160  
 1161  
 1162

1163 We can group the terms that depend on  $\boldsymbol{\lambda}$  and those that do not. Let  $k_g(z) = \sum_{k=m+1}^t \mathbb{I}(z_k = g)$   
 1164 be the number of times lag  $g$  is used in path  $z$ . Then:

1165  
 1166 
$$p(\mathbf{y}_1^t, z \mid \boldsymbol{\lambda}) = \left( \prod_{g=1}^m \lambda_g^{k_g(z)} \right) \left( \prod_{k=m+1}^t \pi(y_{k-z_k}, y_k) \right).$$
  
 1167

1168 Let  $P(\mathbf{y} \mid z) := \prod_{k=m+1}^t \pi(y_{k-z_k}, y_k)$ , which is constant with respect to  $\boldsymbol{\lambda}$ . The prior is given by  
 1169  $p(\boldsymbol{\lambda} \mid \boldsymbol{\alpha}) = \frac{1}{B(\boldsymbol{\alpha})} \prod_{g=1}^m \lambda_g^{\alpha_g-1}$ , where  $B(\boldsymbol{\alpha})$  is the multivariate beta function. Substituting these  
 1170 into the expression for the posterior:

1171  
 1172 
$$\begin{aligned} p(\boldsymbol{\lambda} \mid \mathbf{y}_1^t, \boldsymbol{\alpha}) &\propto \left( \sum_z P(\mathbf{y} \mid z) \prod_{g=1}^m \lambda_g^{k_g(z)} \right) \left( \frac{1}{B(\boldsymbol{\alpha})} \prod_{g=1}^m \lambda_g^{\alpha_g-1} \right) \\ 1173 &\propto \sum_z P(\mathbf{y} \mid z) \prod_{g=1}^m \lambda_g^{\alpha_g + k_g(z) - 1}. \end{aligned}$$
  
 1174  
 1175  
 1176  
 1177  
 1178

1179 We recognize that the term  $\prod_g \lambda_g^{(\alpha_g + k_g(z)) - 1}$  is the kernel of a Dirichlet distribution,  $\text{Dir}(\boldsymbol{\lambda} \mid \boldsymbol{\alpha} +$   
 1180  $k(z))$ . We can write it as  $B(\boldsymbol{\alpha} + k(z)) \cdot \text{Dir}(\boldsymbol{\lambda} \mid \boldsymbol{\alpha} + k(z))$ . Thus, the posterior takes the form of a  
 1181 weighted sum of Dirichlet densities:

1182  
 1183 
$$p(\boldsymbol{\lambda} \mid \mathbf{y}_1^t, \boldsymbol{\alpha}) = \sum_z \pi(z) \cdot \text{Dir}(\boldsymbol{\lambda} \mid \boldsymbol{\alpha} + k(z)),$$
  
 1184

1185 where the mixture weights  $\pi(z)$  are the normalized coefficients, which are precisely the true poste-  
 1186 rior probabilities of the latent paths,  $p(Z = z \mid \mathbf{y}_1^t, \boldsymbol{\alpha})$ . This completes the proof.  $\square$   
 1187

1188 From this mixture structure, we can derive an exact identity for the posterior mean.

1188  
 1189 **Proposition 5** (Bayes Mean as Add-Constant-to-Expected-Counts). *The components of the*  
 1190 *Bayesian posterior mean,  $\hat{\lambda}^{\text{Bayes}} = \mathbb{E}[\lambda \mid \mathbf{y}_1^t, \alpha]$ , are given by:*

1191 
$$\hat{\lambda}_g^{\text{Bayes}} = \frac{\alpha_g + \mathbb{E}_{Z \sim \pi}[k_g(Z)]}{\alpha_0 + (t - m)}, \quad (10)$$
  
 1192

1193 where  $\alpha_0 = \sum_j \alpha_j$ , and  $\mathbb{E}_{Z \sim \pi}[k_g(Z)]$  is the posterior expected number of times lag  $g$  was used,  
 1194 which is computationally intractable.

1195 *Proof.* The posterior mean is defined by the integral of  $\lambda$  over its posterior distribution:

1196 
$$\hat{\lambda}^{\text{Bayes}} = \int_{\Delta_{m-1}} \lambda \cdot p(\lambda \mid \mathbf{y}_1^t, \alpha) d\lambda.$$

1197 We substitute the mixture-of-Dirichlets form of the posterior from Proposition 4:

1198 
$$\hat{\lambda}^{\text{Bayes}} = \int_{\Delta_{m-1}} \lambda \cdot \left( \sum_z \pi(z) \cdot \text{Dir}(\lambda \mid \alpha + k(z)) \right) d\lambda.$$

1199 Since the summation is over a finite set of paths  $z$ , we can swap the integral and the summation:

1200 
$$\hat{\lambda}^{\text{Bayes}} = \sum_z \pi(z) \left( \int_{\Delta_{m-1}} \lambda \cdot \text{Dir}(\lambda \mid \alpha + k(z)) d\lambda \right).$$

1201 The term inside the parentheses is the definition of the mean of a Dirichlet distribution with parameter vector  $\beta = \alpha + k(z)$ . The mean of a  $\text{Dir}(\beta)$  distribution is the vector  $\beta/\beta_0$ , where  $\beta_0 = \sum_j \beta_j$ .  
 1202 In our case, the sum of the parameters is:

1203 
$$\sum_{g=1}^m (\alpha_g + k_g(z)) = \left( \sum_g \alpha_g \right) + \left( \sum_g k_g(z) \right) = \alpha_0 + (t - m).$$

1204 Therefore, the inner integral evaluates to the vector  $\frac{\alpha + k(z)}{\alpha_0 + (t - m)}$ . Substituting this back:

1205 
$$\hat{\lambda}^{\text{Bayes}} = \sum_z \pi(z) \frac{\alpha + k(z)}{\alpha_0 + (t - m)}.$$

1206 This expression is an expectation over the posterior distribution of latent paths,  $Z \sim \pi(z)$ . We can  
 1207 write it as:

1208 
$$\hat{\lambda}^{\text{Bayes}} = \mathbb{E}_{Z \sim \pi} \left[ \frac{\alpha + k(Z)}{\alpha_0 + (t - m)} \right].$$

1209 By the linearity of expectation, we can take the expectation inside for each component  $g$ :

1210 
$$\hat{\lambda}_g^{\text{Bayes}} = \frac{\mathbb{E}_{Z \sim \pi}[\alpha_g + k_g(Z)]}{\alpha_0 + (t - m)} = \frac{\alpha_g + \mathbb{E}_{Z \sim \pi}[k_g(Z)]}{\alpha_0 + (t - m)}.$$

1211 This reveals the "add-constant-to-expected-counts" structure of the estimator, completing the proof.  $\square$

## 1228 F APPROXIMATIONS FOR THE MEAN OF THE POSTERIOR DISTRIBUTION

1229 In this section, we outline the methods used to approximate the mean of the posterior distribution  
 1230 over the mixture weights  $\lambda$ .

### 1231 F.1 MARKOV CHAIN MONTE CARLO (MCMC)

1232 Since an analytical solution is unavailable, we approximate the Bayesian predictive distribution  
 1233 using samples from the posterior distribution generated by a Markov Chain Monte Carlo (MCMC)  
 1234 method, specifically **Gibbs sampling**. Gibbs sampling is well-suited for this problem because, while  
 1235 the full posterior is intractable, the conditional posteriors of the parameters and latent variables are  
 1236 simple to sample from.

1237 The procedure involves augmenting the model with latent variables  $Z_1^t = (Z_{m+1}, \dots, Z_t)$ , where  
 1238  $Z_k = g$  indicates that lag  $g$  was used to generate the transition to  $Y_k$ . The Gibbs sampler iteratively  
 1239 draws from the two full conditional distributions:

1242 1. **Sample Latent Variables  $Z$  given Parameters  $\lambda$ :** For a given parameter vector  $\lambda^{(k-1)}$   
 1243 from the previous iteration, we sample each latent variable  $Z_s$  for  $s \in \{m+1, \dots, t\}$  from  
 1244 its categorical conditional posterior:

$$1246 \quad \mathbb{P}(Z_s = g \mid \mathbf{y}_1^t, \lambda^{(k-1)}) = \frac{\lambda_g^{(k-1)} \pi(y_{s-g}, y_s)}{\sum_{h=1}^m \lambda_h^{(k-1)} \pi(y_{s-h}, y_s)}. \quad (11)$$

1248 This provides a complete sampled sequence of lags,  $\mathbf{z}^{(k)} = (z_{m+1}^{(k)}, \dots, z_t^{(k)})$ .

1250 2. **Sample Parameters  $\lambda$  given Latent Variables  $Z$ :** Given the sampled lags  $\mathbf{z}^{(k)}$ , the  
 1251 Dirichlet prior is now conjugate to the complete-data likelihood. We first count the oc-  
 1252 currences of each lag,  $n_g = \sum_{s=m+1}^t \mathbb{I}(z_s^{(k)} = g)$ . The full conditional posterior for  $\lambda$  is a  
 1253 Dirichlet distribution, from which we draw the next sample  $\lambda^{(k)}$ :

$$1254 \quad p(\lambda \mid \mathbf{y}_1^t, \mathbf{z}^{(k)}, \alpha) = \text{Dirichlet}(\lambda \mid \alpha_1 + n_1, \dots, \alpha_m + n_m). \quad (12)$$

1256 After running the sampler for  $K_{\text{total}}$  iterations and discarding an initial burn-in period, we obtain  
 1257 a set of  $K$  samples,  $\{\lambda^{(1)}, \lambda^{(2)}, \dots, \lambda^{(K)}\}$ , that are approximately drawn from the true posterior  
 1258  $p(\lambda \mid \mathbf{y}_1^t, \alpha)$  shown in Equation 4.

1259 The integral in Equation 4 is then approximated via a Monte Carlo average:

$$1261 \quad \hat{p}(Y_{t+1} = j \mid \mathbf{y}_1^t) = \frac{1}{K} \sum_{k=1}^K p(Y_{t+1} = j \mid \mathbf{y}_1^t, \lambda^{(k)}) \\ 1262 \quad = \frac{1}{K} \sum_{k=1}^K \left( \sum_{g=1}^m \lambda_g^{(k)} \pi(y_{t+1-g}, j) \right). \quad (13)$$

1266 This estimate converges to the true Bayes optimal predictive distribution as  $K \rightarrow \infty$ . It represents  
 1267 the theoretical performance limit for inference under the MTD model assumptions, providing a  
 1268 gold-standard benchmark against which other estimators can be compared.

## 1270 G ALGORITHMS FOR MAXIMUM LIKELIHOOD ESTIMATION OF MTD

1272 Maximum Likelihood Estimation (MLE) for the Mixture Transition Distribution (MTD) does not  
 1273 admit a close-form solution therefore iterative optimization algorithms are required. This section  
 1274 details two iterative algorithms suited for this task. We first review the Expectation-Maximization  
 1275 (EM) algorithm, a standard and widely-used method for latent variable models. We then present  
 1276 Mirror Descent (MD), an alternative optimization framework that is central to our work.

### 1278 G.1 EXPECTATION-MAXIMIZATION (EM) ALGORITHM

1279 The Expectation-Maximization (EM) algorithm is a widely-used iterative method for finding Max-  
 1280 imum Likelihood estimates in statistical models with latent variables. In the context of the MTD  
 1281 model, the latent variables correspond to the specific mixture component responsible for generating  
 1282 each observation. The algorithm alternates between two steps: the Expectation (E) step, where it  
 1283 computes the expected log-likelihood with respect to the posterior distribution of the latent variables,  
 1284 and the Maximization (M) step, where it updates the model parameters to maximize this expected  
 1285 value.

1286 Given the latent variables  $\mathbf{Z} = (Z_{m+1}, \dots, Z_n)$ , where each  $Z_t \in \{1, \dots, m\}$ . The variable  $Z_t = g$   
 1287 indicates that the  $g^{\text{th}}$  mixture component (corresponding to lag  $g$ ) was responsible for generating  
 1288 the transition to  $Y_t$  at time  $t$ . The complete data are  $(\mathbf{y}, \mathbf{z})$ .

1289 The likelihood of the complete data  $(\mathbf{y}_{m+1}^n, \mathbf{z}_{m+1}^n)$ , conditional on  $\mathbf{y}_1^m$ , is given by:

$$1291 \quad \mathbb{P}(\mathbf{y}_{m+1}^n, \mathbf{z}_{m+1}^n \mid \mathbf{y}_1^m; \lambda) = \prod_{t=m+1}^n \mathbb{P}(y_t, z_t \mid \mathbf{y}_1^{t-1}; \lambda) \\ 1292 \quad = \prod_{t=m+1}^n \mathbb{P}(Z_t = z_t \mid \mathbf{y}_1^{t-1}; \lambda) \mathbb{P}(y_t \mid Z_t = z_t, \mathbf{y}_1^{t-1}; \lambda).$$

1296 Under the MTD model assumptions:

1297

- 1298  $\mathbb{P}(Z_t = g \mid \mathbf{y}_1^{t-1}; \boldsymbol{\lambda}) = \lambda_g$
- 1299  $\mathbb{P}(y_t \mid Z_t = g, \mathbf{y}_1^{t-1}; \boldsymbol{\lambda}) = \pi(y_{t-g}, y_t)$

1300

1301 Thus,  $\mathbb{P}(y_t, Z_t = g \mid \mathbf{y}_1^{t-1}; \boldsymbol{\lambda}) = \lambda_g \pi(y_{t-g}, y_t)$ . The complete data likelihood becomes:

1302

$$1303 \mathbb{P}(\mathbf{y}_{m+1}^n, \mathbf{z}_{m+1}^n \mid \mathbf{y}_1^m; \boldsymbol{\lambda}) = \prod_{t=m+1}^n \lambda_{z_t} \pi_{z_t}(y_{t-z_t}, y_t).$$

1304

1305 The complete data log-likelihood,  $\ell_c(\boldsymbol{\lambda}; \mathbf{y}, \mathbf{z}) = \log \mathbb{P}(\mathbf{y}_{m+1}^n, \mathbf{z}_{m+1}^n \mid \mathbf{y}_1^m; \boldsymbol{\lambda})$ , is:

1306

$$1307 \ell_c(\boldsymbol{\lambda}; \mathbf{y}, \mathbf{z}) = \sum_{t=m+1}^n \log(\lambda_{z_t} \pi_{z_t}(y_{t-z_t}, y_t))$$

1308

$$1309 = \sum_{t=m+1}^n \sum_{g=1}^m \mathbb{I}(z_t = g) \log(\lambda_g \pi(y_{t-g}, y_t)), \quad (14)$$

1310

1311

1312 where  $\mathbb{I}(\cdot)$  is the indicator function.

1313

## G.2 EM ALGORITHM STEPS

1314 Let  $\boldsymbol{\lambda}^{(k)}$  be the estimate of  $\boldsymbol{\lambda}$  at iteration  $k$ .

1315

1316 **E-Step (Expectation)** The E-step computes the expectation of the complete-data log-likelihood  
1317 equation 14 with respect to the conditional distribution of the latent variables  $\mathbf{Z}$  given the observed  
1318 data  $\mathbf{y}$  and the current parameter estimate  $\boldsymbol{\lambda}^{(k)}$ . This expectation defines the  $Q$  function:

1319

$$1320 Q(\boldsymbol{\lambda} \mid \boldsymbol{\lambda}^{(k)}) = \mathbb{E}_{\mathbf{Z} \mid \mathbf{y}, \boldsymbol{\lambda}^{(k)}} [\ell_c(\boldsymbol{\lambda}; \mathbf{y}, \mathbf{Z})]$$

1321

$$1322 = \mathbb{E} \left[ \sum_{t=m+1}^n \sum_{g=1}^m \mathbb{I}(Z_t = g) \log(\lambda_g \pi(y_{t-g}, y_t)) \mid \mathbf{y}, \boldsymbol{\lambda}^{(k)} \right]$$

1323

$$1324 = \sum_{t=m+1}^n \sum_{g=1}^m \mathbb{E}[\mathbb{I}(Z_t = g) \mid \mathbf{y}, \boldsymbol{\lambda}^{(k)}] \log(\lambda_g \pi(y_{t-g}, y_t)).$$

1325

1326

1327

1328

1329 The core computation is the posterior probability (responsibility) of  $Z_t = g$ :

1330

$$\gamma_t^{(k)}(g) := \mathbb{E}[\mathbb{I}(Z_t = g) \mid \mathbf{y}, \boldsymbol{\lambda}^{(k)}] = \mathbb{P}(Z_t = g \mid \mathbf{y}, \boldsymbol{\lambda}^{(k)}).$$

1331 Due to the MTD model structure, future observations  $\mathbf{y}_{t+1}^n$  are conditionally independent of  $Z_t$  given  
1332  $\mathbf{y}_1^t$ . Thus, the posterior probability simplifies:

1333

$$1334 \mathbb{P}(Z_t = g \mid \mathbf{y}, \boldsymbol{\lambda}^{(k)}) = \mathbb{P}(Z_t = g \mid \mathbf{y}_1^t, \boldsymbol{\lambda}^{(k)}).$$

1335 Using Bayes' theorem:

1336

$$\gamma_t^{(k)}(g) = \mathbb{P}(Z_t = g \mid \mathbf{y}_1^t, \boldsymbol{\lambda}^{(k)})$$

1337

$$1338 = \frac{\mathbb{P}(y_t \mid Z_t = g, \mathbf{y}_1^{t-1}, \boldsymbol{\lambda}^{(k)}) \mathbb{P}(Z_t = g \mid \mathbf{y}_1^{t-1}, \boldsymbol{\lambda}^{(k)})}{\mathbb{P}(y_t \mid \mathbf{y}_1^{t-1}, \boldsymbol{\lambda}^{(k)})}$$

1339

$$1340 = \frac{\pi(y_{t-g}, y_t) \lambda_g^{(k)}}{\sum_{h=1}^m \mathbb{P}(y_t, Z_t = h \mid \mathbf{y}_1^{t-1}, \boldsymbol{\lambda}^{(k)})}$$

1341

$$1342 = \frac{\lambda_g^{(k)} \pi(y_{t-g}, y_t)}{\sum_{h=1}^m \lambda_h^{(k)} \pi_h(y_{t-h}, y_t)}. \quad (15)$$

1343

1344

1345

1346 The E-step involves calculating these responsibilities  $\gamma_t^{(k)}(g)$  for all  $t \in \{m+1, \dots, n\}$  and  $g \in$   
1347  $\{1, \dots, m\}$ . The  $Q$  function is then:

1348

$$1349 Q(\boldsymbol{\lambda} \mid \boldsymbol{\lambda}^{(k)}) = \sum_{t=m+1}^n \sum_{g=1}^m \gamma_t^{(k)}(g) (\log \lambda_g + \log \pi(y_{t-g}, y_t)). \quad (16)$$

1350  
 1351 **M-Step (Maximization)** The M-step finds the parameter values  $\lambda$  that maximize the  $Q$  function  
 1352 equation 16 subject to the constraints  $\lambda_g \geq 0$  and  $\sum_{g=1}^m \lambda_g = 1$ . This gives the updated estimate  
 1353  $\lambda^{(k+1)}$ .  
 1354

$$\lambda^{(k+1)} = \arg \max_{\lambda} Q(\lambda | \lambda^{(k)}).$$

1355 Since the terms  $\log \pi(y_{t-g}, y_t)$  do not depend on  $\lambda$ , we maximize:

$$1356 \quad f(\lambda) = \sum_{t=m+1}^n \sum_{g=1}^m \gamma_t^{(k)}(g) \log \lambda_g = \sum_{g=1}^m \left( \sum_{t=m+1}^n \gamma_t^{(k)}(g) \right) \log \lambda_g.$$

1359 Let  $C_g = \sum_{t=m+1}^n \gamma_t^{(k)}(g)$ . We maximize  $f(\lambda) = \sum_{g=1}^m C_g \log \lambda_g$  subject to  $\sum_{g=1}^m \lambda_g = 1$ . We  
 1360 use a Lagrange multiplier  $\mu$ :

$$1362 \quad \mathcal{L}(\lambda, \mu) = \sum_{g=1}^m C_g \log \lambda_g - \mu \left( \sum_{g=1}^m \lambda_g - 1 \right).$$

1364 Setting partial derivatives to zero:

$$1366 \quad \frac{\partial \mathcal{L}}{\partial \lambda_g} = \frac{C_g}{\lambda_g} - \mu = 0 \implies \lambda_g = \frac{C_g}{\mu}$$

$$1369 \quad \frac{\partial \mathcal{L}}{\partial \mu} = - \left( \sum_{g=1}^m \lambda_g - 1 \right) = 0 \implies \sum_{g=1}^m \lambda_g = 1.$$

1371 Substituting  $\lambda_g = C_g/\mu$  into the constraint yields  $\mu = \sum_{h=1}^m C_h$ . Therefore:

$$1373 \quad \lambda_g = \frac{C_g}{\sum_{h=1}^m C_h} = \frac{\sum_{t=m+1}^n \gamma_t^{(k)}(g)}{\sum_{h=1}^m \sum_{t'=m+1}^n \gamma_{t'}^{(k)}(h)}.$$

1376 The denominator simplifies as  $\sum_{h=1}^m \sum_{t'=m+1}^n \gamma_{t'}^{(k)}(h) = \sum_{t'=m+1}^n \sum_{h=1}^m \gamma_{t'}^{(k)}(h) =$   
 1377  $\sum_{t'=m+1}^n 1 = n - m$ . The M-step update rule is thus:

$$1379 \quad \lambda_g^{(k+1)} = \frac{\sum_{t=m+1}^n \gamma_t^{(k)}(g)}{n - m}. \quad (17)$$

### 1381 G.3 SUMMARY OF THE EM ALGORITHM

1383 The EM algorithm for estimating the mixture weights  $\lambda$  in the MTD model, assuming known transi-  
 1384 tion matrices  $\pi_g$ , proceeds as follows:

- 1386 **Initialization:** Choose initial weights  $\lambda^{(0)} = (\lambda_1^{(0)}, \dots, \lambda_m^{(0)})$  such that  $\lambda_g^{(0)} \geq 0$  for all  
 1387  $g \in \{1, \dots, m\}$  and  $\sum_{g=1}^m \lambda_g^{(0)} = 1$ . Set the iteration counter  $k = 0$ .
- 1389 **E-Step (Expectation):** Compute the responsibilities  $\gamma_t^{(k)}(g)$  for each time point  $t \in$   
 1390  $\{m+1, \dots, n\}$  and each mixture component  $g \in \{1, \dots, m\}$ , using the current parameter  
 1391 estimates  $\lambda^{(k)}$ :

$$1392 \quad \gamma_t^{(k)}(g) = \frac{\lambda_g^{(k)} \pi(y_{t-g}, y_t)}{\sum_{h=1}^m \lambda_h^{(k)} \pi_h(y_{t-h}, y_t)}. \quad (18)$$

- 1395 **M-Step (Maximization):** Update the mixture weights  $\lambda_g^{(k+1)}$  for each component  $g \in$   
 1396  $\{1, \dots, m\}$  using the computed responsibilities:

$$1397 \quad \lambda_g^{(k+1)} = \frac{\sum_{t=m+1}^n \gamma_t^{(k)}(g)}{n - m}. \quad (19)$$

- 1400 **Convergence Check:** If the change in the parameter estimates (e.g.,  $\|\lambda^{(k+1)} - \lambda^{(k)}\|$ )  
 1401 or the change in the observed data log-likelihood (e.g.,  $\ell(\lambda^{(k+1)}; \mathbf{y}) - \ell(\lambda^{(k)}; \mathbf{y})$ , where  
 1402  $\ell(\lambda; \mathbf{y})$  is the observed data log-likelihood) is below a predefined tolerance  $\epsilon$ , stop the  
 1403 algorithm and return  $\hat{\lambda} = \lambda^{(k+1)}$  as the estimated mixture weights. Otherwise, set  $k \leftarrow$   
 $k + 1$  and repeat from Step 2.

1404 G.4 MIRROR DESCENT  
14051406 This appendix provides detailed derivations for Equation (5) and Proposition 2.  
14071408 G.5 DERIVATION OF THE EXPONENTIATED GRADIENT ALGORITHM  
14091410 The Exponentiated Gradient (EG) algorithm is a specific instance of the Mirror Descent (MD) online  
1411 optimization algorithm. We apply it to the problem of maximizing the MTD log-likelihood function,  
1412  $\ell(\boldsymbol{\lambda})$ , with respect to the mixture weights  $\boldsymbol{\lambda} = (\lambda_1, \dots, \lambda_m)$ . The weights are constrained to the  
1413 probability simplex,  $\Delta_{m-1} = \{\boldsymbol{\lambda} \in \mathbb{R}^m \mid \sum_g \lambda_g = 1, \lambda_g \geq 0\}$ .  
14141415 The general MD update step at iteration  $k$  linearizes the objective function around the current esti-  
1416 mate  $\boldsymbol{\lambda}^{(k)}$  and adds a regularization term. The next iterate,  $\boldsymbol{\lambda}^{(k+1)}$ , is found by solving:  
1417

1418 
$$\boldsymbol{\lambda}^{(k+1)} = \arg \max_{\boldsymbol{\lambda} \in \Delta_{m-1}} \left\{ \langle \nabla \ell(\boldsymbol{\lambda}^{(k)}), \boldsymbol{\lambda} \rangle - \frac{1}{\eta} D_{\Psi}(\boldsymbol{\lambda}, \boldsymbol{\lambda}^{(k)}) \right\}, \quad (20)$$
  
1419

1420 where  $\eta > 0$  is the learning rate,  $\nabla \ell(\boldsymbol{\lambda}^{(k)})$  is the gradient of the log-likelihood evaluated at  $\boldsymbol{\lambda}^{(k)}$ ,  
1421 and  $D_{\Psi}$  is the Bregman divergence associated with a potential function  $\Psi$ . For optimization over  
1422 the simplex, the standard choice is the negative entropy potential,  $\Psi(\boldsymbol{\lambda}) = \sum_{g=1}^m \lambda_g \log \lambda_g$ . The  
1423 resulting Bregman divergence is the unnormalized Kullback-Leibler (KL) divergence:  
1424

1425 
$$D_{\Psi}(\boldsymbol{\lambda}, \boldsymbol{\lambda}^{(k)}) = \sum_{g=1}^m \lambda_g \log \frac{\lambda_g}{\lambda_g^{(k)}}. \quad (21)$$
  
1426  
1427

1428 Therefore the optimization problem in Equation (20) becomes:  
1429

1430 
$$\boldsymbol{\lambda}^{(k+1)} = \arg \max_{\boldsymbol{\lambda} \in \Delta_{m-1}} \left\{ \langle \nabla \ell(\boldsymbol{\lambda}^{(k)}), \boldsymbol{\lambda} \rangle - \frac{1}{\eta} \sum_{g=1}^m \lambda_g \log \frac{\lambda_g}{\lambda_g^{(k)}} \right\}. \quad (22)$$
  
1431  
1432

1433 To solve the optimization problem in Eq. 20, we form the Lagrangian with a multiplier  $\mu$  for the  
1434 constraint  $\sum_g \lambda_g = 1$ :  
1435

1436 
$$\mathcal{L}(\boldsymbol{\lambda}, \mu) = \eta \langle \nabla \ell(\boldsymbol{\lambda}^{(k)}), \boldsymbol{\lambda} \rangle - \sum_g \lambda_g \log \frac{\lambda_g}{\lambda_g^{(k)}} - \mu \left( \sum_g \lambda_g - 1 \right). \quad (23)$$
  
1437  
1438

1439 Setting the derivative  $\partial \mathcal{L} / \partial \lambda_g$  to zero yields:  
1440

1441 
$$\eta \nabla_{\lambda} \ell(\boldsymbol{\lambda}^{(k)})_g - \left( \log \frac{\lambda_g}{\lambda_g^{(k)}} + 1 \right) - \mu = 0$$
  
1442  
1443 
$$\log \frac{\lambda_g}{\lambda_g^{(k)}} = \eta \nabla_{\lambda} \ell(\boldsymbol{\lambda}^{(k)})_g - \mu - 1$$
  
1444  
1445 
$$\lambda_g = \lambda_g^{(k)} \exp(\eta \nabla_{\lambda} \ell(\boldsymbol{\lambda}^{(k)})_g) \exp(-\mu - 1).$$
  
1446  
1447

1448 The term  $\exp(-\mu - 1)$  serves as a normalization constant to ensure  $\sum_g \lambda_g = 1$ . This leads directly  
1449 to the EG update rule presented in Equation (5):  
1450

1451 
$$\lambda_g^{(k+1)} = \frac{\lambda_g^{(k)} \exp(\eta \cdot \nabla_{\lambda} \ell(\boldsymbol{\lambda}^{(k)})_g)}{\sum_{h=1}^m \lambda_h^{(k)} \exp(\eta \cdot \nabla_{\lambda} \ell(\boldsymbol{\lambda}^{(k)})_h)}. \quad (5, \text{repeated})$$
  
1452  
1453

1454 G.6 DERIVATION OF THE ONE-STEP MTD ESTIMATOR  
14551456 We now prove Proposition 2 by specializing the EG update to the MTD model and evaluating it at  
1457 the uniform prior  $\boldsymbol{\lambda}^{(0)} = (1/m, \dots, 1/m)$ .  
1458

1458 **Step 1: MTD Log-Likelihood and its Gradient.** Given an observed sequence prefix  $\mathbf{y}_1^t$ , the MTD  
 1459 log-likelihood is:

$$1460 \quad \ell(\boldsymbol{\lambda}) = \log p(\mathbf{y}_1^t \mid \boldsymbol{\lambda}) = \sum_{k=m+1}^t \log \left( \sum_{h=1}^m \lambda_h \pi(y_{k-h}, y_k) \right). \quad (24)$$

1463 The  $g$ -th component of its gradient is:

$$1465 \quad \nabla_{\lambda} \ell(\boldsymbol{\lambda})_g = \frac{\partial \ell(\boldsymbol{\lambda})}{\partial \lambda_g} = \sum_{k=m+1}^t \frac{\pi(y_{k-g}, y_k)}{\sum_{h=1}^m \lambda_h \pi(y_{k-h}, y_k)}. \quad (25)$$

1468 **Step 2: Evaluate Gradient at the Uniform Prior.** We evaluate this gradient at  $\boldsymbol{\lambda}^{(0)} =$   
 1469  $(1/m, \dots, 1/m)$ :

$$1471 \quad \nabla_{\lambda} \ell(\boldsymbol{\lambda}^{(0)})_g = \sum_{k=m+1}^t \frac{\pi(y_{k-g}, y_k)}{\sum_{h=1}^m (1/m) \pi(y_{k-h}, y_k)} \\ 1472 \quad = m \sum_{k=m+1}^t \frac{\pi(y_{k-g}, y_k)}{\sum_{h=1}^m \pi(y_{k-h}, y_k)}. \quad (26)$$

1477 We recognize the term inside the summation as the posterior responsibility of lag  $g$  under the uniform  
 1478 model:

$$1479 \quad \gamma_k(g) := p(Z_k = g \mid \mathbf{y}_1^t, \boldsymbol{\lambda}^{(0)}) \quad (27)$$

$$1481 \quad = \frac{p(y_k \mid y_{k-g}) p(Z_k = g \mid \boldsymbol{\lambda}^{(0)})}{\sum_h p(y_k \mid y_{k-h}) p(Z_k = h \mid \boldsymbol{\lambda}^{(0)})} \quad (28)$$

$$1483 \quad = \frac{\pi(y_{k-g}, y_k) \cdot (1/m)}{\sum_h \pi(y_{k-h}, y_k) \cdot (1/m)} \quad (29)$$

$$1486 \quad = \frac{\pi(y_{k-g}, y_k)}{\sum_{h=1}^m \pi(y_{k-h}, y_k)}. \quad (30)$$

1487 Thus, the gradient at the uniform prior is a scaled sum of these responsibilities:

$$1489 \quad \nabla_{\lambda} \ell(\boldsymbol{\lambda}^{(0)})_g = m \sum_{k=m+1}^t \gamma_k^{\text{unif}}(g). \quad (31)$$

1492 **Step 3: Apply the EG Update Rule.** Finally, we substitute  $\lambda_g^{(0)} = 1/m$  and the derived gradient  
 1493 into the EG update rule (Eq. 5) to find  $\lambda_g^{(1)}$ :

$$1495 \quad \hat{\lambda}_g^{\text{MD}} = \lambda_g^{(1)} = \frac{\lambda_g^{(0)} \exp(\eta \cdot \nabla_{\lambda} \ell(\boldsymbol{\lambda}^{(0)})_g)}{\sum_{j=1}^m \lambda_j^{(0)} \exp(\eta \cdot \nabla_{\lambda} \ell(\boldsymbol{\lambda}^{(0)})_j)} \\ 1497 \quad = \frac{(1/m) \cdot \exp\left(\eta \cdot m \sum_{k=m+1}^t \gamma_k^{\text{unif}}(g)\right)}{\sum_{j=1}^m (1/m) \cdot \exp\left(\eta \cdot m \sum_{k=m+1}^t \gamma_k^{\text{unif}}(j)\right)} \\ 1500 \quad = \frac{\exp\left(\eta m \sum_{k=m+1}^t \gamma_k^{\text{unif}}(g)\right)}{\sum_{j=1}^m \exp\left(\eta m \sum_{k=m+1}^t \gamma_k^{\text{unif}}(j)\right)}. \quad (32)$$

1505 This completes the proof of Proposition 2.

## 1508 H ONE-STEP MD AS A FIRST-ORDER BAYESIAN APPROXIMATION

1510 In this section, we formally establish a theoretical connection between the one-step Mirror Descent  
 1511 (MD) estimator and the true Bayesian posterior mean. We demonstrate that their respective first-  
 order Taylor expansions around a state of “no evidence” are identical up to a scalar constant. This

1512 result provides a rigorous basis for understanding the one-step MD estimator as a principled approximation  
 1513 to the Bayes-optimal predictor, particularly in a low-data or low-signal regime.

1514 The analysis hinges on treating both estimators as functions of the log-likelihood gradient evaluated  
 1515 at the center of the simplex,  $\mathbf{g} := \nabla_{\lambda} \ell(\lambda^{(0)})$ , and expanding them around the point of no evidence,  
 1516  $\mathbf{g} = \mathbf{0}$ . The approximations will be expressed using Landau notation, where a vector function  
 1517  $\mathbf{f}(\mathbf{g}) = O(\|\mathbf{g}\|^p)$  signifies that  $\|\mathbf{f}(\mathbf{g})\| \leq C\|\mathbf{g}\|^p$  for some constant  $C$  in a neighborhood of  $\mathbf{g} = \mathbf{0}$ .

1518 **Proposition 6** (First-Order Approximation of the One-Step MD Estimator). *Let  $\hat{\lambda}^{MD}(\mathbf{g})$  be the one-  
 1519 step MD estimator defined as  $\hat{\lambda}^{MD}(\mathbf{g}) = \text{softmax}(\eta\mathbf{g})$ , viewed as a function of the log-likelihood  
 1520 gradient  $\mathbf{g}$ . Its first-order Taylor expansion around  $\mathbf{g} = \mathbf{0}$  is given by:*

$$1522 \quad 1523 \quad \hat{\lambda}_k^{MD}(\mathbf{g}) = \frac{1}{m} + \frac{\eta}{m}(g_k - \bar{g}) + O(\|\mathbf{g}\|^2), \quad (33)$$

1524 where  $\bar{g} = \frac{1}{m} \sum_{j=1}^m g_j$ . In vector form, this is  $\hat{\lambda}^{MD}(\mathbf{g}) = \lambda^{(0)} + \frac{\eta}{m} \text{Proj}_{\Delta}(\mathbf{g}) + O(\|\mathbf{g}\|^2)$ , where  
 1525  $\lambda^{(0)} = (1/m, \dots, 1/m)$  and  $\text{Proj}_{\Delta}$  is the operator that projects a vector onto the hyperplane of  
 1526 vectors that sum to zero.

1527 *Proof.* The one-step MD update is given by the softmax function,  $\hat{\lambda}_k^{MD}(\mathbf{g}) = \frac{\exp(\eta g_k)}{\sum_{j=1}^m \exp(\eta g_j)}$ . Since  
 1528 the exponential function is analytic, the softmax function is also analytic in  $\mathbf{g}$ , and its Taylor series  
 1529 expansion around  $\mathbf{g} = \mathbf{0}$  exists. The expansion is given by:

$$1530 \quad 1531 \quad \hat{\lambda}^{MD}(\mathbf{g}) = \hat{\lambda}^{MD}(\mathbf{0}) + J_{\hat{\lambda}^{MD}}(\mathbf{0})\mathbf{g} + O(\|\mathbf{g}\|^2),$$

1532 where  $J_{\hat{\lambda}^{MD}}(\mathbf{0})$  is the Jacobian matrix of  $\hat{\lambda}^{MD}(\mathbf{g})$  evaluated at  $\mathbf{g} = \mathbf{0}$ .

1533 **Zeroth-Order Term:** At  $\mathbf{g} = \mathbf{0}$ , the estimator evaluates to the uniform distribution, which is the  
 1534 prior mean  $\lambda^{(0)}$ :

$$1535 \quad 1536 \quad \hat{\lambda}_k^{MD}(\mathbf{0}) = \frac{\exp(0)}{\sum_{j=1}^m \exp(0)} = \frac{1}{m} = \lambda_k^{(0)}.$$

1537 **First-Order Term (Jacobian):** The entries of the Jacobian matrix,  $J_{k,j}(\mathbf{g}) = \frac{\partial}{\partial g_j} \hat{\lambda}_k^{MD}(\mathbf{g})$ , are given  
 1538 by  $\eta \cdot \hat{\lambda}_k^{MD}(\mathbf{g})(\delta_{kj} - \hat{\lambda}_j^{MD}(\mathbf{g}))$ . Evaluating at  $\mathbf{g} = \mathbf{0}$ , where  $\hat{\lambda}_j^{MD}(\mathbf{0}) = 1/m$  for all  $j$ :

$$1539 \quad 1540 \quad \frac{\partial \hat{\lambda}_k^{MD}}{\partial g_j} \Big|_{\mathbf{g}=\mathbf{0}} = \eta \cdot \frac{1}{m} \left( \delta_{kj} - \frac{1}{m} \right).$$

1541 **Assembling the Expansion:** The  $k$ -th component of the expansion is  $\hat{\lambda}_k^{MD}(\mathbf{g}) = \hat{\lambda}_k^{MD}(\mathbf{0}) +$   
 1542  $\sum_{j=1}^m \frac{\partial \hat{\lambda}_k^{MD}}{\partial g_j} \Big|_{\mathbf{0}} \cdot g_j + O(\|\mathbf{g}\|^2)$ :

$$1543 \quad 1544 \quad \begin{aligned} \hat{\lambda}_k^{MD}(\mathbf{g}) &= \frac{1}{m} + \sum_{j=1}^m \left[ \frac{\eta}{m} \left( \delta_{kj} - \frac{1}{m} \right) \right] g_j + O(\|\mathbf{g}\|^2) \\ 1545 &= \frac{1}{m} + \frac{\eta}{m} \left( \sum_{j=1}^m \delta_{kj} g_j - \frac{1}{m} \sum_{j=1}^m g_j \right) + O(\|\mathbf{g}\|^2) \\ 1546 &= \frac{1}{m} + \frac{\eta}{m}(g_k - \bar{g}) + O(\|\mathbf{g}\|^2). \end{aligned}$$

1547 This completes the proof. □

1548 Next, we derive the corresponding approximation for the Bayesian posterior mean. We linearize the  
 1549 log-likelihood around the prior mean,  $\lambda^{(0)}$ , which allows for an analytical treatment of the posterior.

1550 **Proposition 7** (First-Order Approximation of the Bayesian Posterior Mean). *Consider a Bayesian  
 1551 model with a uniform Dirichlet(1) prior over  $\lambda \in \Delta_{m-1}$  and a log-likelihood linearized around*

1566 the prior mean,  $\ell(\boldsymbol{\lambda}) = \ell(\boldsymbol{\lambda}^{(0)}) + \langle \mathbf{g}, \boldsymbol{\lambda} - \boldsymbol{\lambda}^{(0)} \rangle$ . The resulting posterior mean,  $\hat{\boldsymbol{\lambda}}^{\text{Bayes}}(\mathbf{g})$ , has a  
 1567 first-order Taylor expansion around  $\mathbf{g} = \mathbf{0}$  given by:  
 1568

$$1569 \hat{\lambda}_k^{\text{Bayes}}(\mathbf{g}) = \frac{1}{m} + \frac{1}{m(m+1)}(g_k - \bar{g}) + O(\|\mathbf{g}\|^2). \quad (34)$$

1571 In vector form, this is  $\hat{\boldsymbol{\lambda}}^{\text{Bayes}}(\mathbf{g}) = \boldsymbol{\lambda}^{(0)} + \text{Cov}_{\boldsymbol{\lambda}^{(0)}}(\boldsymbol{\lambda})\mathbf{g} + O(\|\mathbf{g}\|^2)$ , where  $\text{Cov}_{\boldsymbol{\lambda}^{(0)}}(\boldsymbol{\lambda})$  is the co-  
 1572 variance matrix of the prior distribution.  
 1573

1574 *Proof.* Under the linearized likelihood, the posterior density is  $p(\boldsymbol{\lambda}|\mathbf{g}) \propto p(\boldsymbol{\lambda}) \exp(\ell(\boldsymbol{\lambda})) \propto$   
 1575  $\exp(\langle \mathbf{g}, \boldsymbol{\lambda} \rangle)$ , where terms constant in  $\boldsymbol{\lambda}$  are absorbed into the normalization constant. The poste-  
 1576 rior mean is:  
 1577

$$1578 \hat{\boldsymbol{\lambda}}^{\text{Bayes}}(\mathbf{g}) = \frac{\int_{\Delta_{m-1}} \boldsymbol{\lambda} \cdot \exp(\langle \mathbf{g}, \boldsymbol{\lambda} \rangle) d\mu(\boldsymbol{\lambda})}{\int_{\Delta_{m-1}} \exp(\langle \mathbf{g}, \boldsymbol{\lambda} \rangle) d\mu(\boldsymbol{\lambda})},$$

1580 where  $d\mu(\boldsymbol{\lambda})$  is the uniform probability measure over the simplex  $\Delta_{m-1}$ . Let  $N_k(\mathbf{g})$  be the numer-  
 1581 ator's  $k$ -th component and  $Z(\mathbf{g})$  be the denominator. The function  $\hat{\boldsymbol{\lambda}}^{\text{Bayes}}(\mathbf{g})$  is analytic, allowing a  
 1582 Taylor expansion.  
 1583

1584 **Zeroth-Order Term:** At  $\mathbf{g} = \mathbf{0}$ , the exponential term is 1. The posterior equals the prior, so the  
 1585 posterior mean is the prior mean:  
 1586

$$1587 \hat{\boldsymbol{\lambda}}^{\text{Bayes}}(\mathbf{0}) = \frac{\int_{\Delta_{m-1}} \boldsymbol{\lambda} d\mu(\boldsymbol{\lambda})}{\int_{\Delta_{m-1}} 1 d\mu(\boldsymbol{\lambda})} = \mathbb{E}_{\boldsymbol{\lambda} \sim \text{Dir}(\mathbf{1})}[\boldsymbol{\lambda}] = \boldsymbol{\lambda}^{(0)}.$$

1590 **First-Order Term (Jacobian):** The Jacobian entries are  $\frac{\partial \hat{\lambda}_k}{\partial g_j} = \frac{\partial}{\partial g_j} \left( \frac{N_k}{Z} \right)$ . Using the quotient rule:  
 1591

$$1592 \frac{\partial \hat{\lambda}_k}{\partial g_j} = \frac{1}{Z^2} \left( Z \frac{\partial N_k}{\partial g_j} - N_k \frac{\partial Z}{\partial g_j} \right).$$

1595 We find the required derivatives of  $N_k(\mathbf{g})$  and  $Z(\mathbf{g})$  differentiating under the integral sign, which is  
 1596 applicable here as the integrands are continuous on the compact domain  $\Delta_{m-1}$ :  
 1597

$$1598 \frac{\partial Z}{\partial g_j} = \frac{\partial}{\partial g_j} \int_{\Delta_{m-1}} \exp \left( \sum_i g_i \lambda_i \right) d\mu(\boldsymbol{\lambda}) = \int_{\Delta_{m-1}} \lambda_j \exp \left( \sum_i g_i \lambda_i \right) d\mu(\boldsymbol{\lambda})$$

$$1601 \frac{\partial N_k}{\partial g_j} = \frac{\partial}{\partial g_j} \int_{\Delta_{m-1}} \lambda_k \exp \left( \sum_i g_i \lambda_i \right) d\mu(\boldsymbol{\lambda}) = \int_{\Delta_{m-1}} \lambda_k \lambda_j \exp \left( \sum_i g_i \lambda_i \right) d\mu(\boldsymbol{\lambda})$$

1603 Now, we evaluate these components at  $\mathbf{g} = \mathbf{0}$ :  
 1604

- 1605 •  $Z(\mathbf{0}) = \int 1 d\mu(\boldsymbol{\lambda}) = 1$ .
- 1606 •  $N_k(\mathbf{0}) = \int \lambda_k d\mu(\boldsymbol{\lambda}) = \mathbb{E}[\lambda_k] = 1/m$ .
- 1609 •  $\frac{\partial Z}{\partial g_j} \Big|_{\mathbf{g}=\mathbf{0}} = \int_{\Delta_{m-1}} \lambda_j \exp(\langle \mathbf{0}, \boldsymbol{\lambda} \rangle) d\mu(\boldsymbol{\lambda}) = \int \lambda_j d\mu(\boldsymbol{\lambda}) = \mathbb{E}[\lambda_j] = 1/m$ .
- 1612 •  $\frac{\partial N_k}{\partial g_j} \Big|_{\mathbf{g}=\mathbf{0}} = \int_{\Delta_{m-1}} \lambda_k \lambda_j \exp(\langle \mathbf{0}, \boldsymbol{\lambda} \rangle) d\mu(\boldsymbol{\lambda}) = \int \lambda_k \lambda_j d\mu(\boldsymbol{\lambda}) = \mathbb{E}[\lambda_k \lambda_j]$ .

1615 Substituting these evaluated terms into the quotient rule expression at  $\mathbf{g} = \mathbf{0}$ :

$$1617 \frac{\partial \hat{\lambda}_k}{\partial g_j} \Big|_{\mathbf{g}=\mathbf{0}} = \frac{1 \cdot \mathbb{E}[\lambda_k \lambda_j] - (1/m) \cdot (1/m)}{1^2} = \mathbb{E}[\lambda_k \lambda_j] - \mathbb{E}[\lambda_k] \mathbb{E}[\lambda_j] = \text{Cov}_{\boldsymbol{\lambda}^{(0)}}(\lambda_k, \lambda_j).$$

1619 This establishes that the Jacobian of the posterior mean at  $\mathbf{g} = \mathbf{0}$  is the prior covariance matrix.

1620 **Assembling the Expansion:** For a Dirichlet(1) distribution, the covariance matrix is  $\text{Cov}(\lambda_k, \lambda_j) =$   
 1621  $\frac{m\delta_{kj}-1}{m^2(m+1)}$ . The  $k$ -th component of the expansion is:  
 1622

$$\begin{aligned} 1623 \hat{\lambda}_k^{\text{Bayes}}(\mathbf{g}) &= \frac{1}{m} + \sum_{j=1}^m \frac{m\delta_{kj}-1}{m^2(m+1)} g_j + O(\|\mathbf{g}\|^2) \\ 1624 &= \frac{1}{m} + \frac{1}{m^2(m+1)} \left( mg_k - \sum_{j=1}^m g_j \right) + O(\|\mathbf{g}\|^2) \\ 1625 &= \frac{1}{m} + \frac{m}{m^2(m+1)} (g_k - \bar{g}) + O(\|\mathbf{g}\|^2) \\ 1626 &= \frac{1}{m} + \frac{1}{m(m+1)} (g_k - \bar{g}) + O(\|\mathbf{g}\|^2). \\ 1627 \\ 1628 \\ 1629 \\ 1630 \\ 1631 \\ 1632 \\ 1633 \end{aligned}$$

1634 This completes the proof of the proposition.  $\square$   
 1635

1636 By comparing the results of Proposition 6 and Proposition 7, we arrive at our main result.  
 1637

1638 **Theorem 3** (First-Order Equivalence of the Estimators). *Let  $\hat{\lambda}^{\text{MD}}(\mathbf{g}; \eta)$  be the one-step MD estimator  
 1639 with learning rate  $\eta$ , and let  $\hat{\lambda}^{\text{Bayes}}(\mathbf{g})$  be the Bayesian posterior mean under the linearized  
 1640 likelihood. There exists a unique learning rate  $\eta = \frac{1}{m+1}$  for which the two estimators are first-order  
 1641 equivalent at  $\mathbf{g} = \mathbf{0}$ .*

1642 *Proof.* Two estimators are first-order equivalent at  $\mathbf{g} = \mathbf{0}$  if their values and their Jacobian matrices  
 1643 are identical at that point. As shown in Propositions 6 and 7, the first condition,  $\hat{\lambda}^{\text{MD}}(\mathbf{0}; \eta) =$   
 1644  $\hat{\lambda}^{\text{Bayes}}(\mathbf{0})$ , holds for any  $\eta$ . The equivalence thus depends on matching their Jacobians.  
 1645

1646 From the proof of Proposition 6, the Jacobian of the MD estimator at  $\mathbf{g} = \mathbf{0}$  is:  
 1647

$$1648 J_{\hat{\lambda}^{\text{MD}}}(\mathbf{0}) = \frac{\eta}{m} \left( \mathbf{I} - \frac{1}{m} \mathbf{1} \mathbf{1}^T \right). \\ 1649$$

1650 From the proof of Proposition 7, the Jacobian of the Bayesian posterior mean is:  
 1651

$$1652 J_{\hat{\lambda}^{\text{Bayes}}}(\mathbf{0}) = \frac{1}{m(m+1)} \left( \mathbf{I} - \frac{1}{m} \mathbf{1} \mathbf{1}^T \right). \\ 1653$$

1654 Equating the two Jacobians,  $J_{\hat{\lambda}^{\text{MD}}}(\mathbf{0}) = J_{\hat{\lambda}^{\text{Bayes}}}(\mathbf{0})$ , requires their scalar coefficients to be equal,  
 1655 since the matrix factor is non-zero for  $m > 1$ :  
 1656

$$1657 \frac{\eta}{m} = \frac{1}{m(m+1)}. \\ 1658$$

1659 Solving for  $\eta$  yields the unique solution  $\eta = \frac{1}{m+1}$ .  $\square$   
 1660

1661 This theorem provides a theoretical justification for the performance of the one-step MD estimator.  
 1662 It demonstrates that this simple, non-iterative update is not merely a heuristic but a principled, first-  
 1663 order approximation of the Bayesian posterior mean under a linearized likelihood.  
 1664

1665 **Remark (The Role of  $\eta$  and the Small-Gradient Assumption).** The first-order equivalence es-  
 1666 tablished in Theorem 3 holds in the regime where  $\|\mathbf{g}\| \rightarrow 0$ , as this is where the higher-order terms,  
 1667  $O(\|\mathbf{g}\|^2)$ , are negligible. For many models, the gradient's magnitude,  $\|\mathbf{g}\|$ , scales with the amount  
 1668 of data (e.g., sequence length  $T$ ), which appears to invalidate the approximation when the data size  
 1669 is large.

1670 However, the one-step MD estimator,  $\hat{\lambda}^{\text{MD}} = \text{softmax}(\eta \mathbf{g})$ , can remain a well-behaved estimator  
 1671 even for large  $\|\mathbf{g}\|$  if  $\eta$  is scaled appropriately. The term  $\eta \mathbf{g}$  determines the softmax behavior. If we  
 1672 set the learning rate to be inversely proportional to the signal strength, for instance  $\eta(T) = \Theta(1/T)$ ,  
 1673 the norm of the argument,  $\|\eta \mathbf{g}\|$ , can remain bounded. This scaling prevents the softmax output  
 from saturating and allows the estimator to remain sensitive to the information in  $\mathbf{g}$ .

1674 On the Bayesian side, under the linearized likelihood, the posterior mean  $\hat{\lambda}^{\text{Bayes}}(\mathbf{g})$  lacks a scaling  
 1675 parameter analogous to  $\eta$ . For large  $\|\mathbf{g}\|$ , the posterior density  $\exp(\langle \mathbf{g}, \boldsymbol{\lambda} \rangle)$  concentrates sharply at  
 1676 the vertex of the simplex maximizing the inner product with  $\mathbf{g}$ . In this case, the first-order approxi-  
 1677 mation from Proposition 7 breaks down as the neglected  $O(\|\mathbf{g}\|^2)$  term becomes dominant.

1678 The equivalence in Theorem 3 should therefore be interpreted as a local consistency result at  $\mathbf{g} = \mathbf{0}$ .  
 1679 It shows that for low-signal scenarios, the MD update is a principled approximation to the Bayesian  
 1680 one, and it provides a theoretically grounded value for  $\eta$  in that regime. The empirical success of the  
 1681 one-step estimator for large  $T$  suggests that while the functional forms of the two estimators diverge  
 1682 beyond the first order, a properly tuned MD estimator may still serve as an effective proxy for the  
 1683 Bayesian posterior mean, motivating analytical frameworks beyond local Taylor expansions.  
 1684

## 1685 I LEARNING-RATE SCALING VIA A LIPSCHITZ (SMOOTHNESS) CONSTANT 1686

1687 In our main analysis, we established a first-order equivalence between the one-step MD estimator  
 1688 and the Bayesian posterior mean in the regime of "no evidence," where the log-likelihood gradient  
 1689  $\mathbf{g} = \mathbf{0}$ . However, for a sequence of length  $T$ , the magnitude of the gradient,  $\|\mathbf{g}\|$ , typically scales  
 1690 with  $T$ . This raises the question of how the learning rate of the one-step MD estimator,  $\hat{\lambda}^{\text{MD}} =$   
 1691  $\text{softmax}(\eta \mathbf{g})$  should be scaled with  $T$  to maintain good performance.  
 1692

1693 In this section, we provide a theoretical justification for scaling the learning rate as  $\eta = \Theta(1/T)$ . We  
 1694 demonstrate that the negative log-likelihood function, viewed as a loss function over the simplex,  
 1695 has a gradient that is Lipschitz continuous with a constant  $L$  that grows linearly with the sequence  
 1696 length  $T$ . Standard optimization theory suggests setting the learning rate inversely proportional to  
 1697 this Lipschitz constant, i.e.,  $\eta \propto 1/L$ , to ensure stable updates. We use the same notation as the  
 1698 before:  
 1699

$$c_{t,g} = \pi(y_{t-g}, y_t), \quad t = m+1, \dots, T, \quad g = 1, \dots, m,$$

1700 and  $m$  is the number of lags.

1701 **Assumption.** We assume there exists a constant

$$c_{\min} > 0$$

1703 such that for every  $t \in \{m+1, \dots, T\}$  and every  $g \in \{1, \dots, m\}$ ,

$$c_{t,g} = \pi(y_{t-g}, y_t) \geq c_{\min}. \quad (35)$$

1705 Because each  $c_{t,g}$  is a conditional probability, we also have the trivial upper bound  
 1706

$$c_{t,g} \leq 1 \quad \text{for all } t, g. \quad (36)$$

1707 Under these assumptions the denominators that appear in derivatives are uniformly bounded away  
 1708 from zero, and global, uniform bounds on the Hessian are valid.

1709 **Lemma 1** (Hessian decomposition). *For  $\ell(\boldsymbol{\lambda}) = \sum_{t=m+1}^T \log(\sum_{g=1}^m \lambda_g c_{t,g})$  the Hessian satisfies*

$$1713 \nabla^2 \ell(\boldsymbol{\lambda}) = - \sum_{t=m+1}^T \frac{\mathbf{c}_t \mathbf{c}_t^\top}{(\sum_{g=1}^m \lambda_g c_{t,g})^2}, \quad \mathbf{c}_t := (c_{t,1}, \dots, c_{t,m})^\top.$$

1716 Hence the Hessian of the negative log-likelihood  $f(\boldsymbol{\lambda}) = -\ell(\boldsymbol{\lambda})$  is

$$1718 \nabla^2 f(\boldsymbol{\lambda}) = \sum_{t=m+1}^T \frac{\mathbf{c}_t \mathbf{c}_t^\top}{(\sum_{g=1}^m \lambda_g c_{t,g})^2}.$$

1721 *Proof.* Direct differentiation of  $\ell(\boldsymbol{\lambda})$  yields the displayed formulas.  $\square$

1723 Write  $s_t(\boldsymbol{\lambda}) := \sum_{g=1}^m \lambda_g c_{t,g}$  and consequently the Hessian of the loss is

$$1725 \nabla^2 f(\boldsymbol{\lambda}) = \sum_{t=m+1}^T \frac{\mathbf{c}_t \mathbf{c}_t^\top}{s_t(\boldsymbol{\lambda})^2}. \quad (37)$$

1727 Each summand in equation 37 is a rank-one positive semi-definite matrix.

1728 I.1 UNIFORM OPERATOR-NORM BOUND ON THE HESSIAN  
17291730 We now derive a uniform bound on the spectral (operator) norm of  $\nabla^2 f(\lambda)$  that depends linearly on  
1731  $T - m$ .1732 **Lemma 2** (Operator-norm bound). *Under the standing assumption equation 35 (and equation 36),*  
1733 *for every  $\lambda$  in the full simplex  $\Delta_{m-1} = \{\lambda \geq 0, \sum_g \lambda_g = 1\}$  we have*

1734  
1735 
$$\|\nabla^2 f(\lambda)\|_{\text{op}} \leq (T - m) \frac{m}{c_{\min}^2}. \quad (38)$$
  
1736

1737 *Proof.* From equation 37 and subadditivity of the operator norm,  
1738

1739  
1740 
$$\|\nabla^2 f(\lambda)\|_{\text{op}} = \left\| \sum_{t=m+1}^T \frac{\mathbf{c}_t \mathbf{c}_t^\top}{s_t(\lambda)^2} \right\|_{\text{op}} \leq \sum_{t=m+1}^T \frac{\|\mathbf{c}_t \mathbf{c}_t^\top\|_{\text{op}}}{s_t(\lambda)^2}.$$
  
1741

1742 For a rank-one matrix  $\mathbf{u} \mathbf{u}^\top$  the operator norm equals  $\|\mathbf{u}\|_2^2$ . Hence  
1743

1744  
1745 
$$\|\mathbf{c}_t \mathbf{c}_t^\top\|_{\text{op}} = \|\mathbf{c}_t\|_2^2 = \sum_{g=1}^m c_{t,g}^2.$$
  
1746

1747 Using equation 36 we get the upper bound  $\|\mathbf{c}_t\|_2^2 \leq m \cdot 1^2 = m$  for every  $t$ .1748 For the denominator, by equation 35 and since  $\sum_{g=1}^m \lambda_g = 1$ ,

1749  
1750 
$$s_t(\lambda) = \sum_{g=1}^m \lambda_g c_{t,g} \geq \sum_{g=1}^m \lambda_g c_{\min} = c_{\min}.$$
  
1751

1752 Therefore for every  $t$ ,

1753  
1754 
$$\frac{\|\mathbf{c}_t \mathbf{c}_t^\top\|_{\text{op}}}{s_t(\lambda)^2} \leq \frac{m}{c_{\min}^2}.$$
  
1755

1756 Summing over  $t = m+1, \dots, T$  yields  
1757

1758  
1759 
$$\|\nabla^2 f(\lambda)\|_{\text{op}} \leq \sum_{t=m+1}^T \frac{m}{c_{\min}^2} = (T - m) \frac{m}{c_{\min}^2},$$
  
1760

1761 which is the bound equation 38. □  
17621763 I.2 IMPROVED BOUND AT THE CENTER OF THE SIMPLEX  
17641765 Here we show that evaluating exactly at the uniform vector  $\lambda^*$  yields a strictly better constant: the  
1766 spectral norm of the Hessian at  $\lambda^*$  is bounded by  $(T - m) m^2$ . This gives a less pessimistic Lipschitz  
1767 constant and hence a looser restriction on the conservative step-size  $\eta$ .1768 **Proposition 8** (Operator-norm bound at the uniform vector). *Let  $\lambda^* = (1/m, \dots, 1/m)$ . For the*  
1769 *loss  $f(\lambda) = -\ell(\lambda)$  we have*

1770  
1771 
$$\|\nabla^2 f(\lambda^*)\|_{\text{op}} \leq (T - m) m^2. \quad (39)$$

1772 *In particular, the gradient  $\nabla f$  is Lipschitz at  $\lambda^*$  with constant  $L^* \leq (T - m) m^2$ , and the conser-*  
1773 *vative step-size choice  $\eta \leq 1/L^*$  yields  $\eta = \Theta(1/T)$  for fixed  $m$ .*1774 *Proof.* Recall the Hessian decomposition (Eq. equation 37):  
1775

1776  
1777 
$$\nabla^2 f(\lambda) = \sum_{t=m+1}^T \frac{\mathbf{c}_t \mathbf{c}_t^\top}{s_t(\lambda)^2}, \quad \mathbf{c}_t = (c_{t,1}, \dots, c_{t,m})^\top, \quad s_t(\lambda) = \sum_{g=1}^m \lambda_g c_{t,g}.$$
  
1778

1779 Evaluate at the uniform vector  $\lambda^*$ . Then

1780  
1781 
$$s_t(\lambda^*) = \frac{1}{m} \sum_{g=1}^m c_{t,g} =: \frac{S_t}{m}, \quad S_t := \sum_{g=1}^m c_{t,g}.$$

1782 Hence the  $t$ -th summand becomes  
 1783

$$\frac{\mathbf{c}_t \mathbf{c}_t^\top}{s_t(\boldsymbol{\lambda}^*)^2} = \frac{\mathbf{c}_t \mathbf{c}_t^\top}{(S_t/m)^2} = \frac{m^2}{S_t^2} \mathbf{c}_t \mathbf{c}_t^\top.$$

1786 Taking operator norms and using subadditivity,  
 1787

$$\|\nabla^2 f(\boldsymbol{\lambda}^*)\|_{\text{op}} \leq \sum_{t=m+1}^T \frac{m^2}{S_t^2} \|\mathbf{c}_t \mathbf{c}_t^\top\|_{\text{op}}.$$

1792 For each  $t$ ,  $\|\mathbf{c}_t \mathbf{c}_t^\top\|_{\text{op}} = \|\mathbf{c}_t\|_2^2$ . Observe the elementary inequality  
 1793

$$\|\mathbf{c}_t\|_2^2 \leq \left( \sum_{g=1}^m c_{t,g} \right)^2 = S_t^2,$$

1797 which holds because  $(\sum_i a_i)^2 = \sum_i a_i^2 + 2 \sum_{i < j} a_i a_j \geq \sum_i a_i^2$  for nonnegative  $a_i$ . Using this  
 1798 inequality we obtain, for every  $t$ ,

$$\frac{m^2}{S_t^2} \|\mathbf{c}_t\|_2^2 \leq \frac{m^2}{S_t^2} S_t^2 = m^2.$$

1802 Summing over  $t = m+1, \dots, T$  yields  
 1803

$$\|\nabla^2 f(\boldsymbol{\lambda}^*)\|_{\text{op}} \leq \sum_{t=m+1}^T m^2 = (T-m) m^2,$$

1804 which proves equation 39. The remaining claims follow immediately from the standard equivalence  
 1805 between Hessian operator-norm bounds and local Lipschitz continuity of the gradient, and the  
 1806 reciprocal step-size rule  $\eta \leq 1/L^*$ .  $\square$   
 1807

1811 **Theorem 4** (Lipschitz gradient and  $\eta$  scaling at the uniform mixture). *At the uniform vector  $\boldsymbol{\lambda}^* =$   
 1812  $(1/m, \dots, 1/m)$  the loss  $f(\boldsymbol{\lambda}) = -\ell(\boldsymbol{\lambda})$  is  $L^*$ -smooth with*  
 1813

$$L^* \leq (T-m) m^2. \quad (40)$$

1814 Consequently, the conservative step-size rule  $\eta \leq \frac{1}{L^*}$  yields the asymptotic scaling  
 1815

$$\eta = \Theta\left(\frac{1}{T}\right) \quad (41)$$

1816 for fixed  $m$ .  
 1817

1822 *Proof.* Proposition 8 establishes that at  $\boldsymbol{\lambda}^*$  the Hessian satisfies  
 1823

$$\|\nabla^2 f(\boldsymbol{\lambda}^*)\|_{\text{op}} \leq (T-m) m^2.$$

1824 By the standard equivalence between bounded Hessian operator norm and gradient Lipschitz continuity,  
 1825 this implies  $\nabla f$  is  $L^*$ -Lipschitz at  $\boldsymbol{\lambda}^*$  with  $L^*$  as in equation 40. The conservative step-size  
 1826 choice  $\eta \leq 1/L^*$  is therefore sufficient to guarantee stability of gradient-based updates (and analogously  
 1827 for mirror descent / exponentiated-gradient after translating to the mirror geometry). Since  
 1828  $T-m = \Theta(T)$ , the scaling  $\eta = \Theta(1/T)$  follows for fixed  $m$ .  $\square$   
 1829

1831 The assumption equation 35 (strict positivity of every transition probability appearing in the likelihood)  
 1832 is the minimal condition that guarantees a *uniform* finite Lipschitz constant  $L$  over the entire  
 1833 simplex  $\Delta_{m-1}$ . If some transitions were zero, then for parameter vectors placing mass on  
 1834 coordinates corresponding to zero transitions some denominators  $s_t(\boldsymbol{\lambda})$  could vanish and the Hessian  
 1835 operator norm would be unbounded (hence no global  $L$  exists).

1836 **J ASYMPTOTIC PROPERTIES OF THE LIKELIHOOD GRADIENT**

1837  
1838 In this section, we study the asymptotic properties of the gradient of the log-likelihood function. We  
1839 are mostly interested in the asymptotic scaling of the gradient with the sequence length  $T$ .

1840  
1841 **Lemma 3** (Asymptotic Properties of the Gradient). *Let the true parameter  $\lambda^* \in \text{int}(\Delta_{m-1})$  induce*  
1842 *a Markov chain on the history space  $\mathcal{Y}^m$  that is aperiodic and irreducible on a finite state space.*  
1843 *This implies the chain is geometrically ergodic. Let  $\mathbb{E}_{\lambda^*}^{\text{stat}}$  denote expectation with respect to the*  
1844 *stationary distribution of this chain. The mean of the score vector  $\mathbf{g}(\mathbf{Y})$  exhibits the following*  
1845 *asymptotic properties as  $N_{\text{obs}} \rightarrow \infty$ : The expected score vector scales linearly with  $N_{\text{obs}} = T - m$ :*

1846 
$$\mathbf{g}_0(\lambda^*) := \mathbb{E}_{\lambda^*}[\mathbf{g}(\mathbf{Y})] = N_{\text{obs}} \cdot \mathbf{v}(\lambda^*) + O(1), \quad (42)$$

1847 where  $\mathbf{v}(\lambda^*)$  is the constant vector of stationary expected single-step scores, whose  $h$ -th component  
1848 is:

1849 
$$[\mathbf{v}(\lambda^*)]_h = m \cdot \mathbb{E}_{\lambda^*}^{\text{stat}} \left[ \frac{\pi(Y_{t-h}, Y_t)}{\sum_{j=1}^m \pi(Y_{t-j}, Y_t)} \right]. \quad (43)$$

1850  
1851 The  $O(1)$  term represents a constant offset due to initial conditions that does not grow with  $N_{\text{obs}}$ .

1852  
1853 *Proof.* Let us first define the score contribution from a single time step  $t$  as the vector  $\mathbf{z}_t(\mathbf{Y}) \in \mathbb{R}^m$ ,  
1854 whose  $h$ -th component is given by:

1855 
$$[\mathbf{z}_t(\mathbf{Y})]_h = m \frac{\pi(Y_{t-h}, Y_t)}{\sum_{j=1}^m \pi(Y_{t-j}, Y_t)}.$$

1856  
1857 The total score vector is the sum of these contributions over the observation period:

1858 
$$\mathbf{g}(\mathbf{Y}) = \sum_{t=m+1}^n \mathbf{z}_t(\mathbf{Y}), \quad \text{where } N_{\text{obs}} = T - m.$$

1859  
1860 The process  $(\mathbf{z}_t)_{t>m}$  is a sequence of random vectors. Because it is a function of the underlying  
1861 ergodic Markov chain  $(Y_{t-m}, \dots, Y_t)$ , the sequence  $(\mathbf{z}_t)$  is also ergodic and its distribution  
1862 converges to a stationary distribution. By the linearity of expectation, the expected score is the sum of  
1863 the individual expectations:

1864 
$$\mathbb{E}_{\lambda^*}[\mathbf{g}(\mathbf{Y})] = \sum_{t=m+1}^n \mathbb{E}_{\lambda^*}[\mathbf{z}_t(\mathbf{Y})].$$

1865  
1866 The key assumption is the geometric ergodicity of the Markov chain. This implies that the distribution  
1867 of the state  $(Y_{t-m}, \dots, Y_t)$  converges exponentially fast to the unique stationary distribution,  
1868 regardless of the initial state  $(Y_1, \dots, Y_m)$ . Consequently, the expectation  $\mathbb{E}_{\lambda^*}[\mathbf{z}_t(\mathbf{Y})]$  converges  
1869 exponentially fast to its stationary-state expectation,  $\mathbf{v}(\lambda^*)$ . This convergence can be quantified.  
1870 There exist a constant vector  $\mathbf{C}$  and a rate  $\rho \in (0, 1)$  such that for all  $t > m$ :

1871 
$$\|\mathbb{E}_{\lambda^*}[\mathbf{z}_t(\mathbf{Y})] - \mathbf{v}(\lambda^*)\| \leq \|\mathbf{C}\| \rho^{t-m}.$$

1872  
1873 We can now rewrite the sum of expectations:

1874 
$$\begin{aligned} \mathbb{E}_{\lambda^*}[\mathbf{g}(\mathbf{Y})] &= \sum_{t=m+1}^n (\mathbf{v}(\lambda^*) + (\mathbb{E}_{\lambda^*}[\mathbf{z}_t(\mathbf{Y})] - \mathbf{v}(\lambda^*))) \\ &= \left( \sum_{t=m+1}^n \mathbf{v}(\lambda^*) \right) + \left( \sum_{t=m+1}^n (\mathbb{E}_{\lambda^*}[\mathbf{z}_t(\mathbf{Y})] - \mathbf{v}(\lambda^*)) \right) \\ &= N_{\text{obs}} \cdot \mathbf{v}(\lambda^*) + \mathbf{E}_n, \end{aligned}$$

1875  
1876 where  $\mathbf{E}_n$  is the cumulative error term due to the process not having reached stationarity at early  
1877 time steps. We can bound the norm of this error term:

1878 
$$\|\mathbf{E}_n\| = \left\| \sum_{t=m+1}^n (\mathbb{E}_{\lambda^*}[\mathbf{z}_t] - \mathbf{v}(\lambda^*)) \right\| \leq \sum_{t=m+1}^n \|\mathbb{E}_{\lambda^*}[\mathbf{z}_t] - \mathbf{v}(\lambda^*)\| \leq \sum_{t=m+1}^n \|\mathbf{C}\| \rho^{t-m}.$$

1890 Let  $k = t - m$ . The sum becomes a geometric series:  
 1891

$$1892 \quad \| \mathbf{E}_n \| \leq \| \mathbf{C} \| \sum_{k=1}^{n-m} \rho^k < \| \mathbf{C} \| \sum_{k=1}^{\infty} \rho^k = \| \mathbf{C} \| \frac{\rho}{1-\rho}.$$

1895 The sum of the error terms is bounded by a finite constant that does not depend on  $n$  or  $N_{\text{obs}}$ .  
 1896 Therefore, the error term is  $O(1)$ . This proves the first claim:  $\mathbf{g}_0(\boldsymbol{\lambda}^*) = N_{\text{obs}} \cdot \mathbf{v}(\boldsymbol{\lambda}^*) + O(1)$ . Note  
 1897 that  $O(1)$  is also  $o(N_{\text{obs}})$ , so the term is asymptotically sub-linear.  $\square$

1898

1899

1900

1901

1902

1903

1904

1905

1906

1907

1908

1909

1910

1911

1912

1913

1914

1915

1916

1917

1918

1919

1920

1921

1922

1923

1924

1925

1926

1927

1928

1929

1930

1931

1932

1933

1934

1935

1936

1937

1938

1939

1940

1941

1942

1943